

Damping ring design

Maxim Korostelev (speaker)

Andy Wolski

Kai Hock

Kosmas Panagiotidis

James Jones

University of Liverpool and the Cockcroft Institute, UK

17 April 2008

Goals for LC-ABD WP2

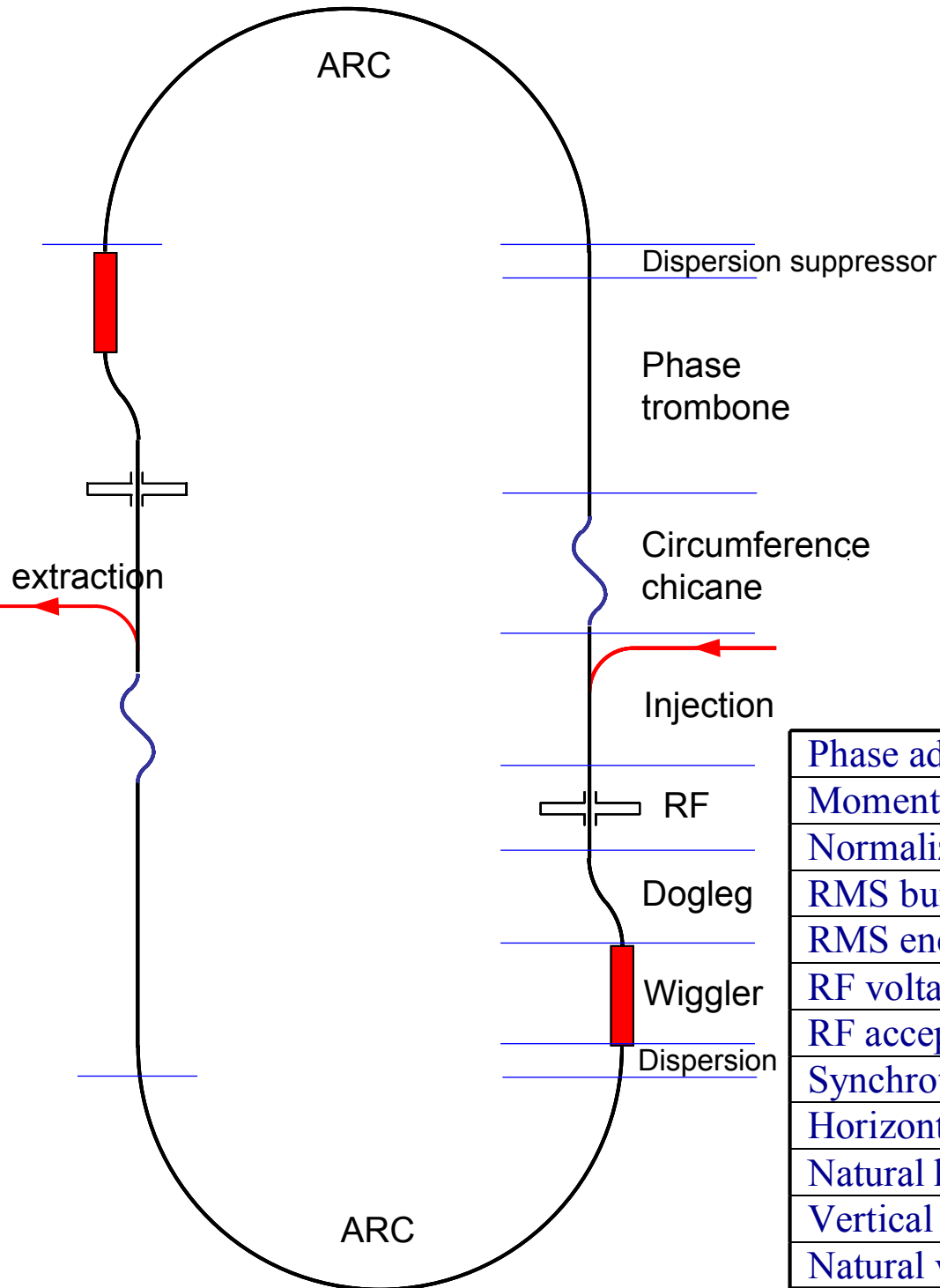
Technical design of vacuum system

Development of impedance model and analysis of beam stability

Low emittance tuning

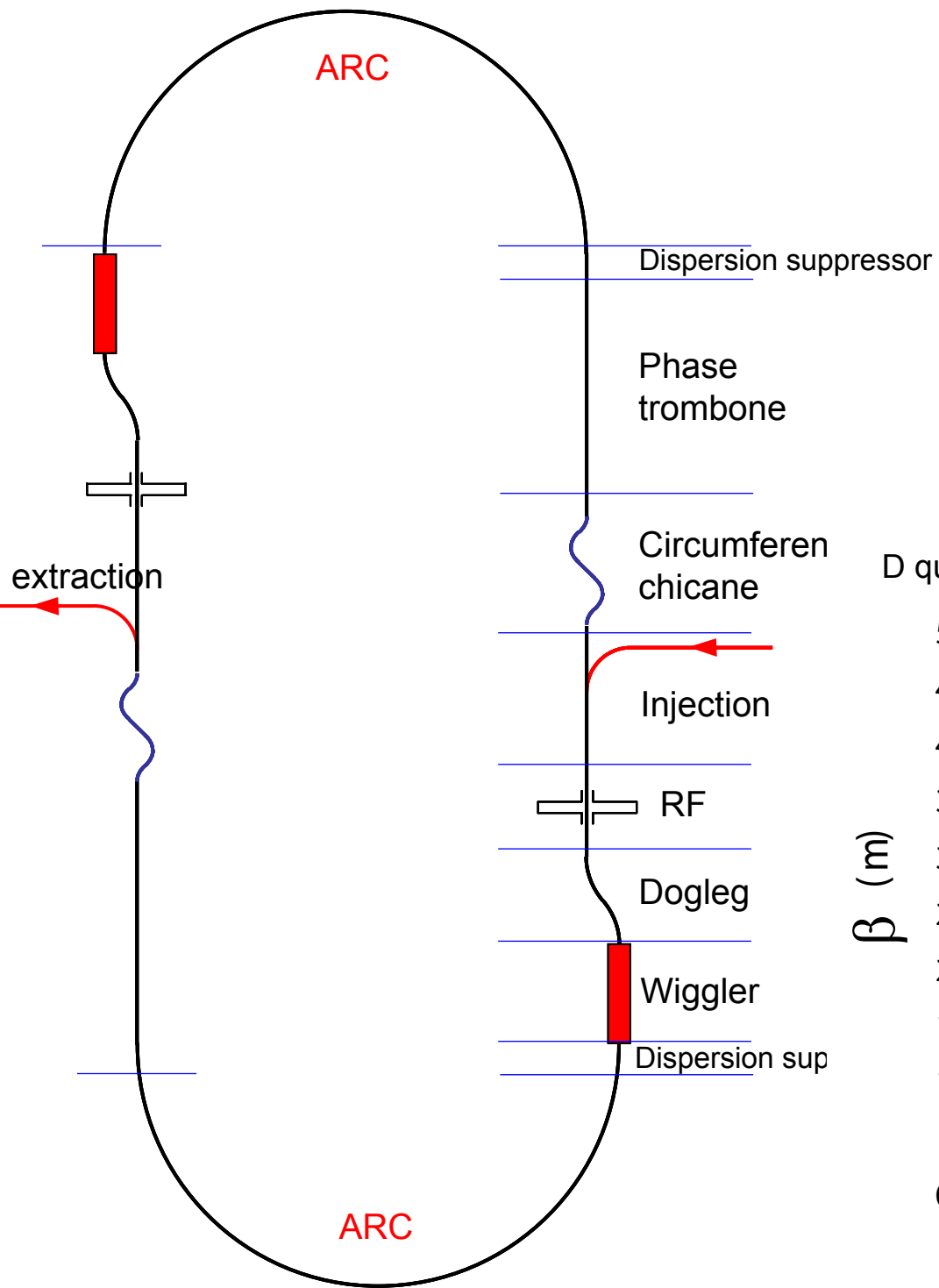
Also done in progress: lattice development & optimization of dynamic aperture

Major Parameters

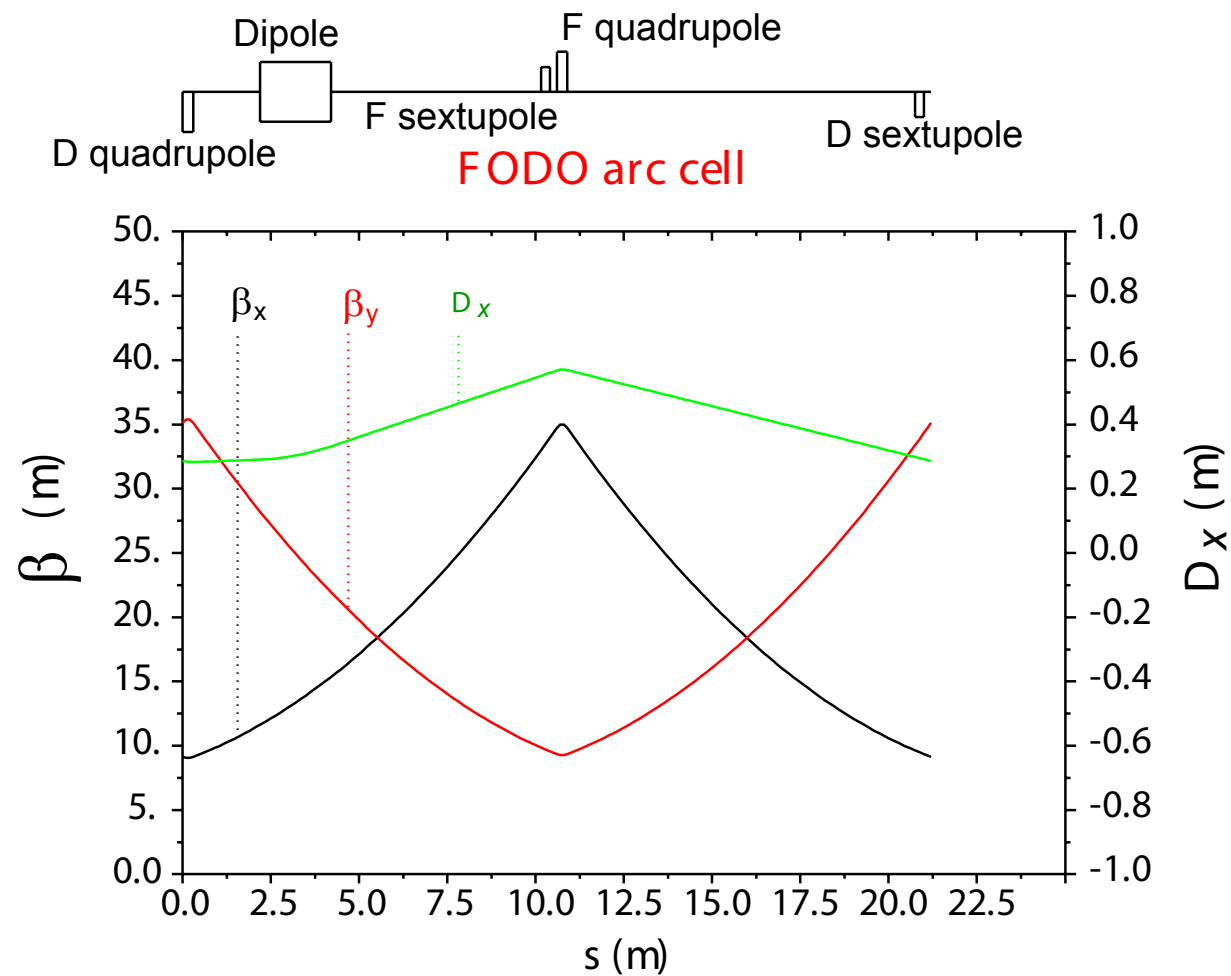


Beam energy	5 GeV
Circumference	6476.44 m
Revolution time	21.6 us
RF frequency	650 MHz
Harmonic number	14042
Type of arc cell	FODO with one dipole
Total length of wigglers	215.6 m
Energy loss per turn	10.3 MeV/turn
Relative damping factor	9.7
Transverse damping time	21.0 ms

	72°	90°	100°
Phase advance per arc cell	72°	90°	100°
Momentum compaction	2.8×10^{-4}	1.7×10^{-4}	1.3×10^{-4}
Normalized horiz. emittance	6.6 μm	4.7 μm	4.3 μm
RMS bunch length	6.0 mm	6.0 mm	6.0 mm
RMS energy spread	1.27×10^{-3}	1.27×10^{-3}	1.27×10^{-3}
RF voltage	31.6 MV	21.1 MV	17.2 MV
RF acceptance	2.35 %	1.99 %	1.72 %
Synchrotron tune	0.061	0.038	0.028
Horizontal betatron tune	64.12	75.12	78.12
Natural horiz. chromaticity	-68.3	-95.1	-105.4
Vertical betatron tune	61.41	71.41	75.41
Natural vert. chromaticity	-67.8	-93.4	-104.0



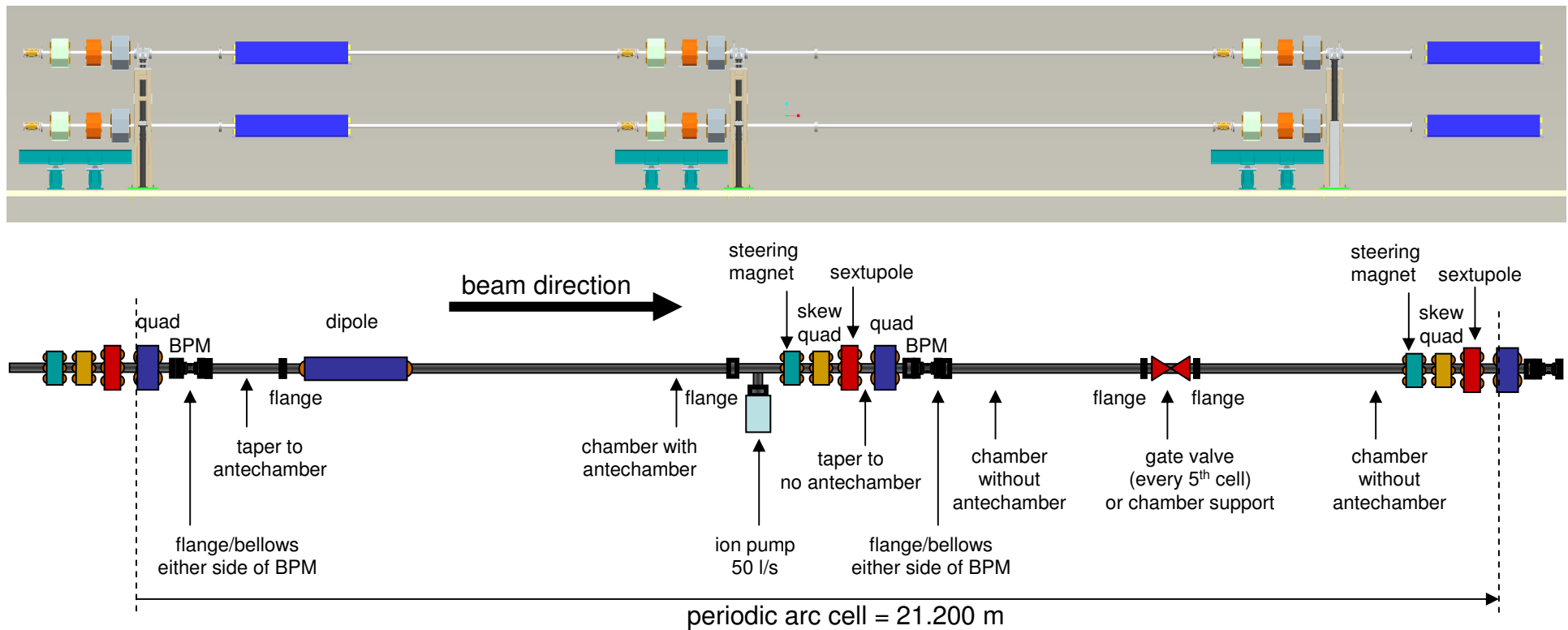
Arc FODO cell length	21.2 m
Arc dipole length	2.0 m
Number of FODO cells	192
Total number of sextupoles	384
Maximum sextupole gradient	215 T/m ²
Arc dipole field	0.273 T





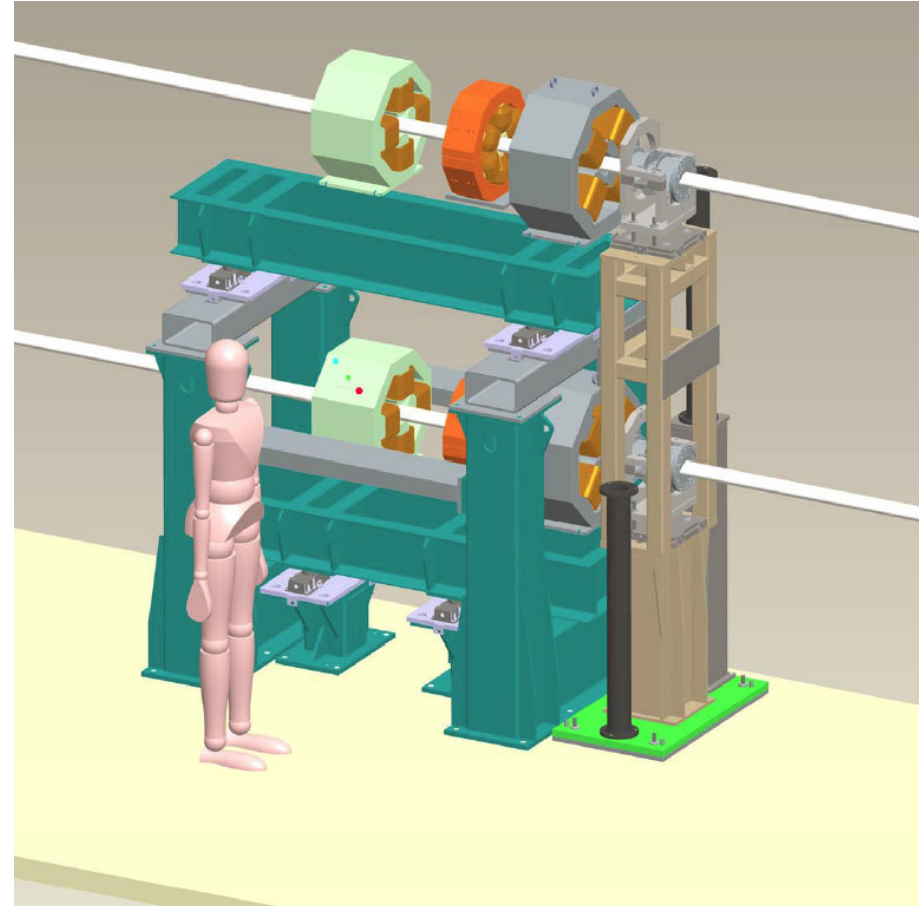
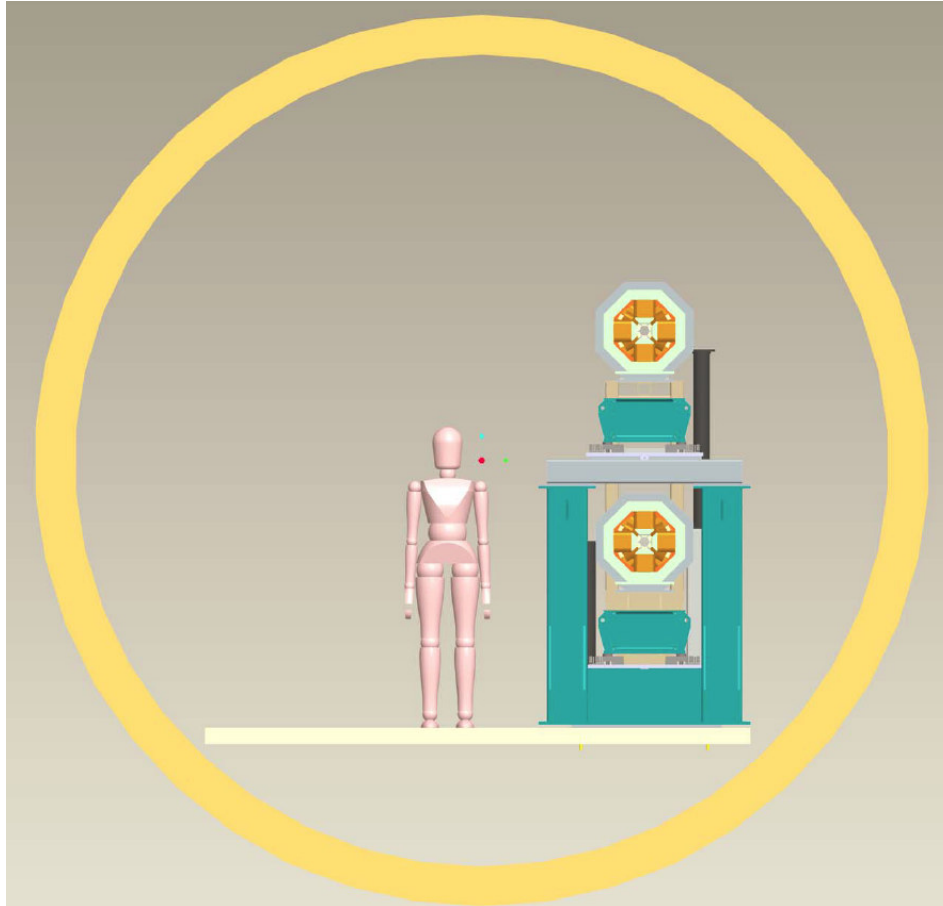
Arc Cell: Vacuum System Concept

- NEG coating provides most of the pumping.
- Antechamber downstream of dipoles reduces synchrotron radiation in main chamber.
- BPMs shielded from synchrotron radiation by tapers.
- BPMs separately supported and "isolated" from rest of chamber through bellows.
- Bellows occur roughly every 10 m (appropriate for bake-out/activation).
- **Single dipole per arc cell** simplifies design and reduces cost (minimizes tapers etc.)



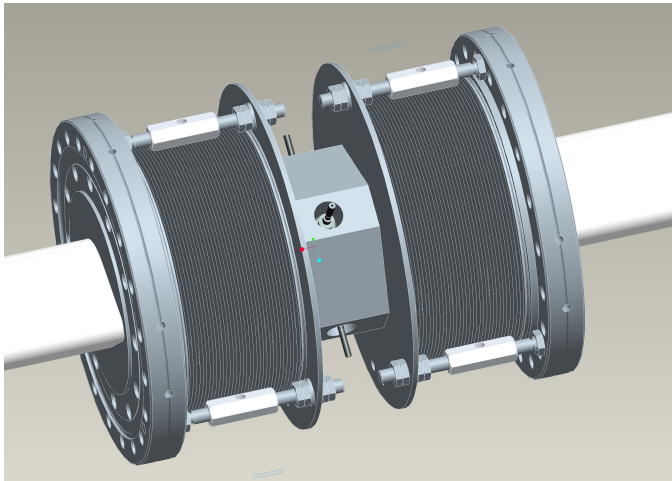


Magnet and BPM Supports

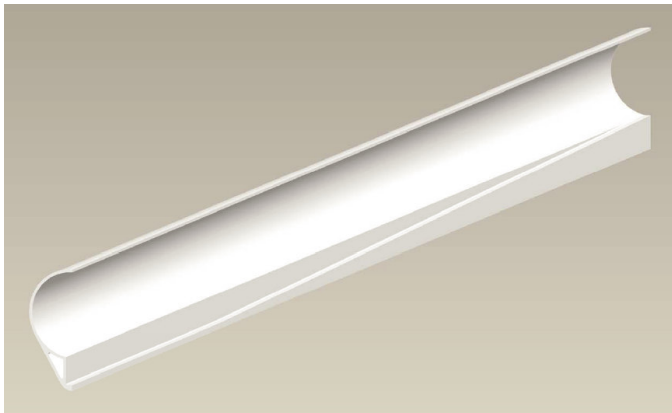




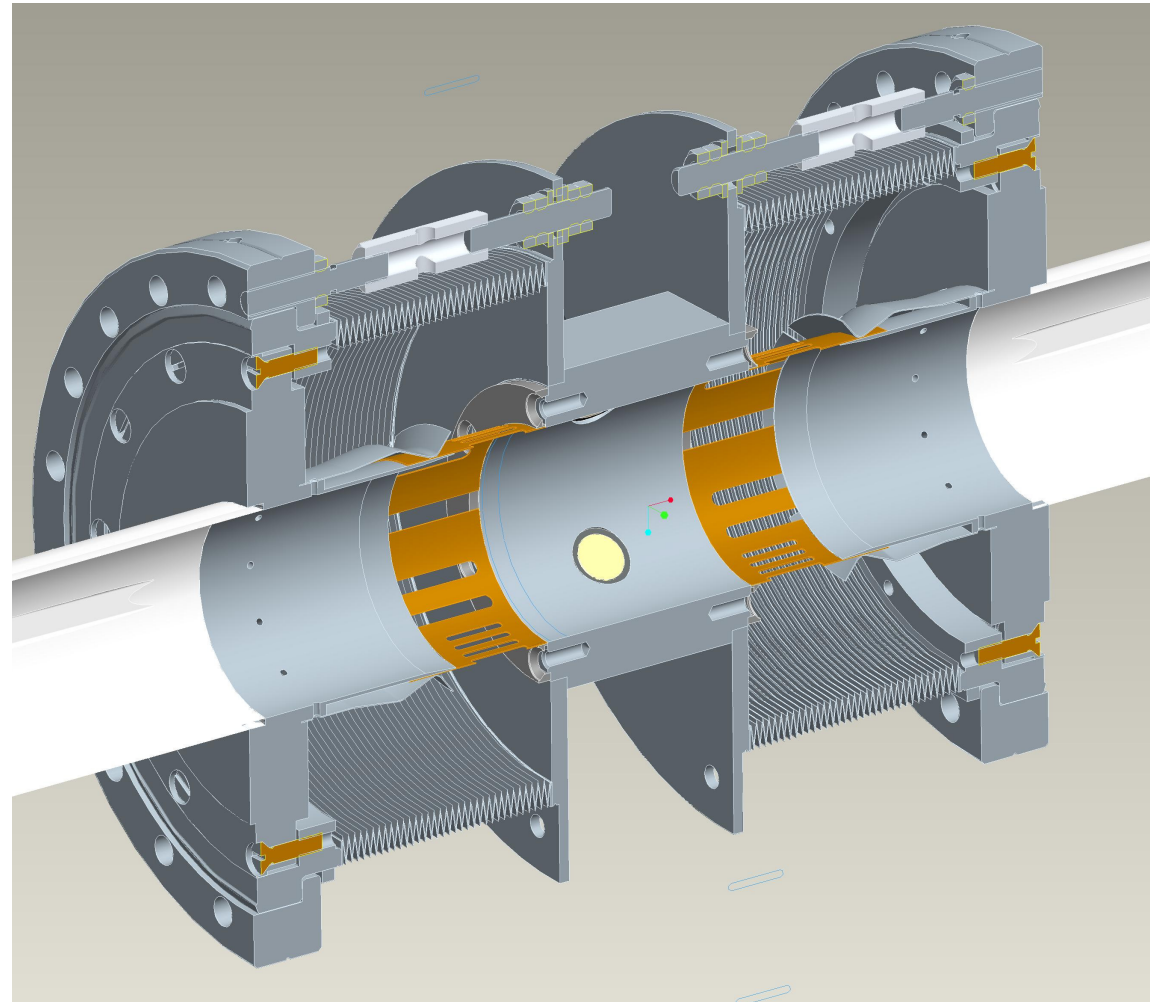
BPM Chambers



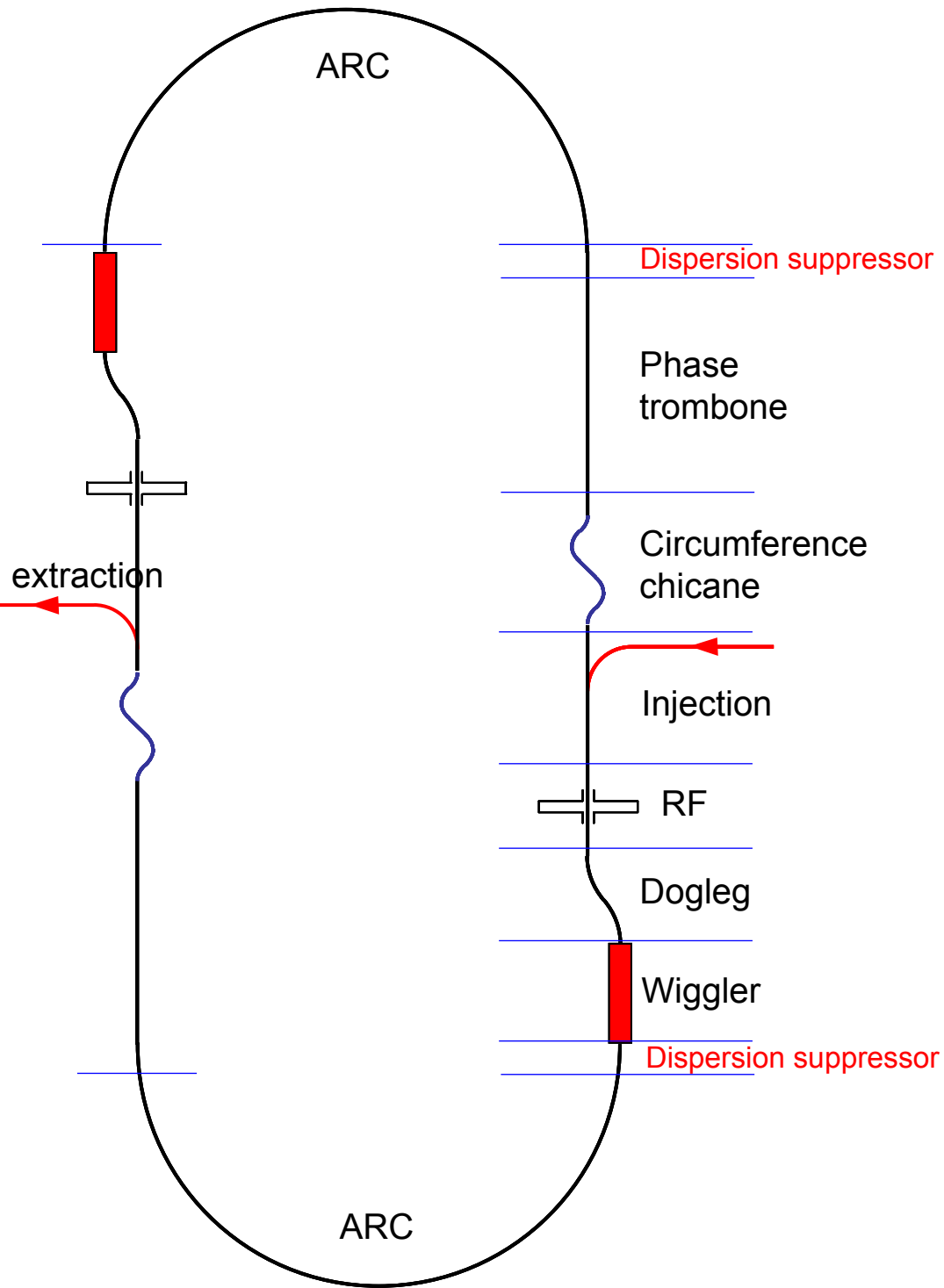
Bellows/BPM external view



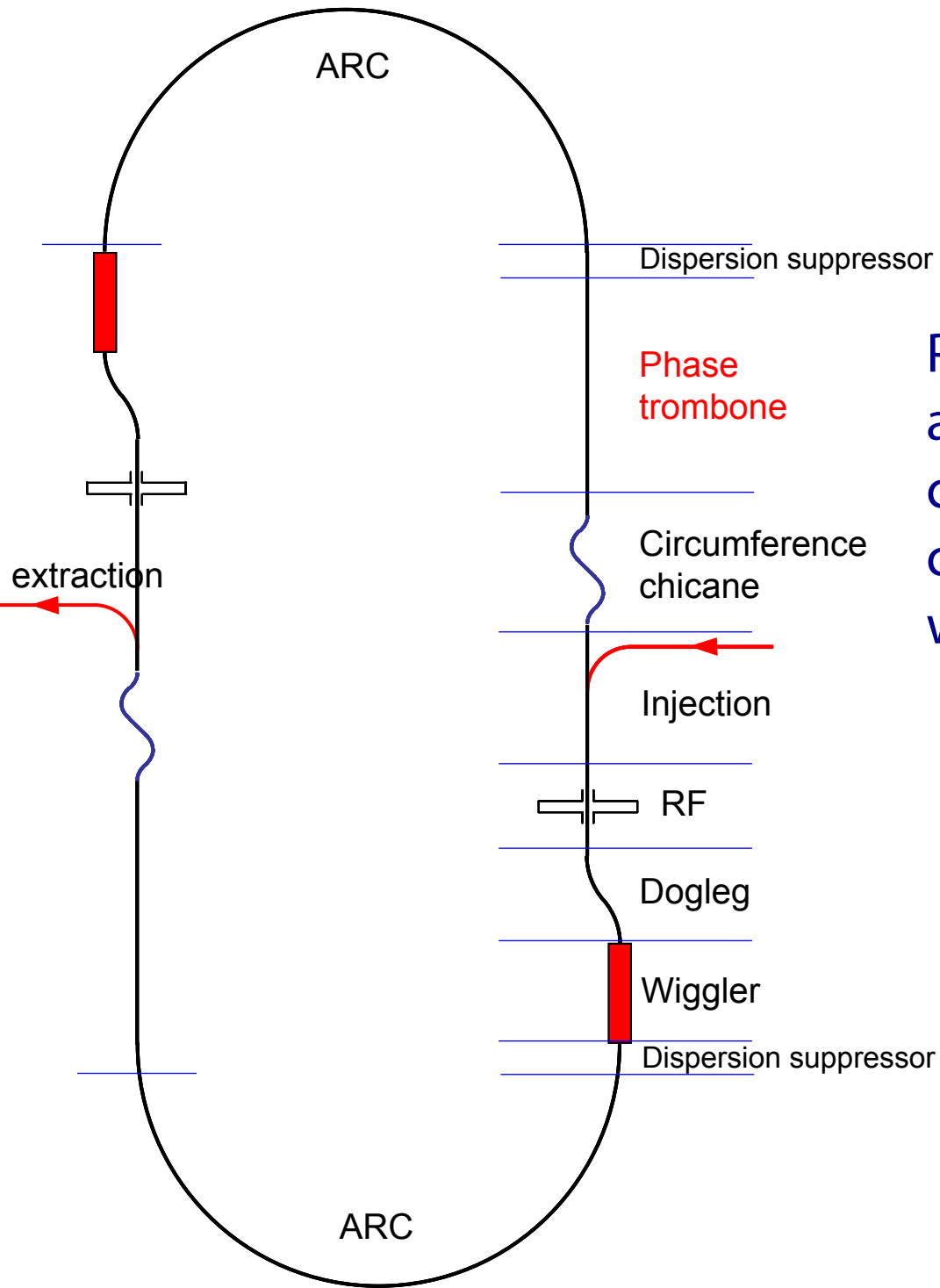
Antechamber taper (into BPM chamber)



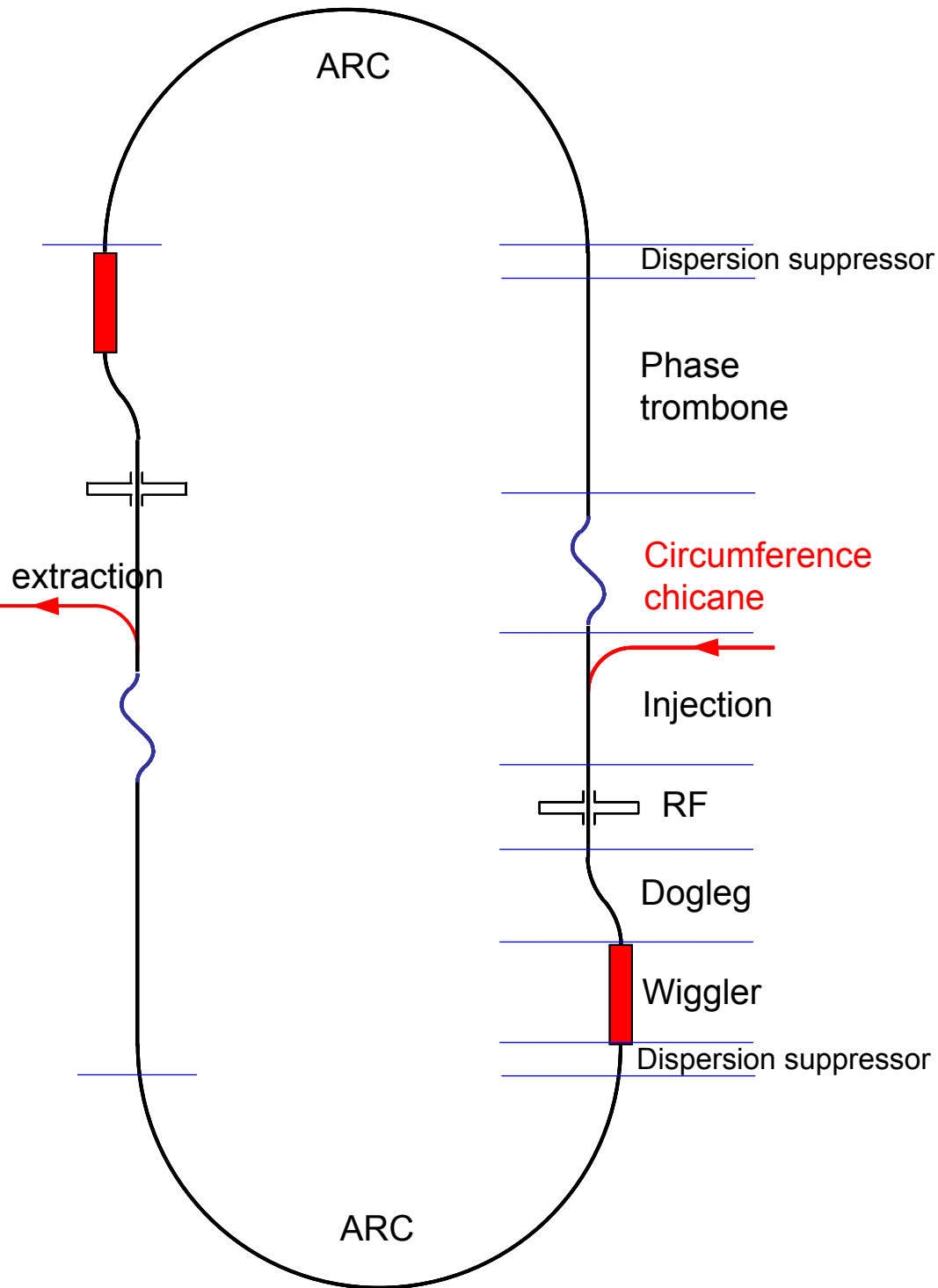
Bellows/BPM internal view



Dispersion suppressors in the ends of the arc are used to cancel the horizontal dispersion in the straight sections.

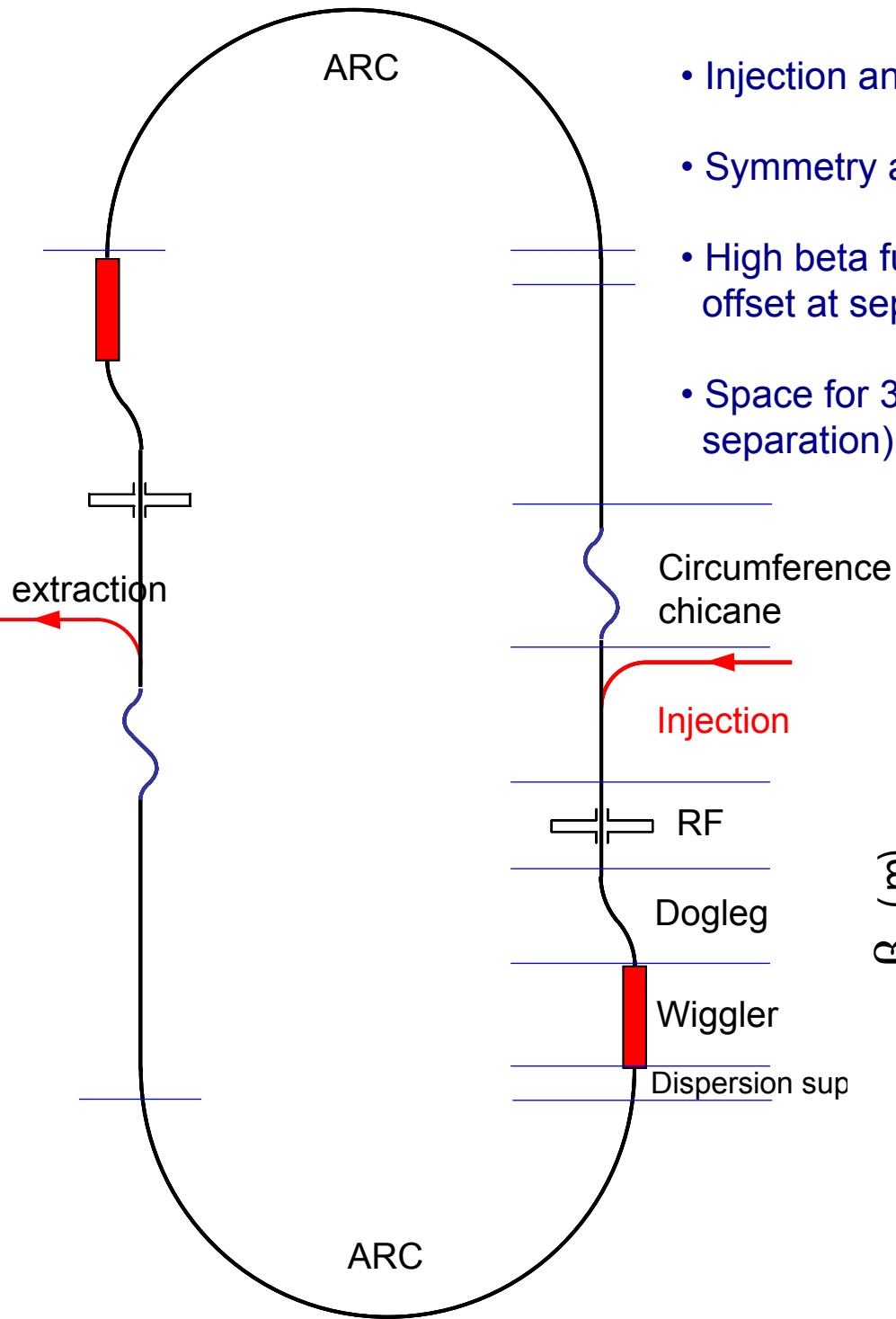


Phase trombone allows to vary phase advance per the straight section without change of the optics in the chicane, RF cavities, injection/extraction section and wigglers.

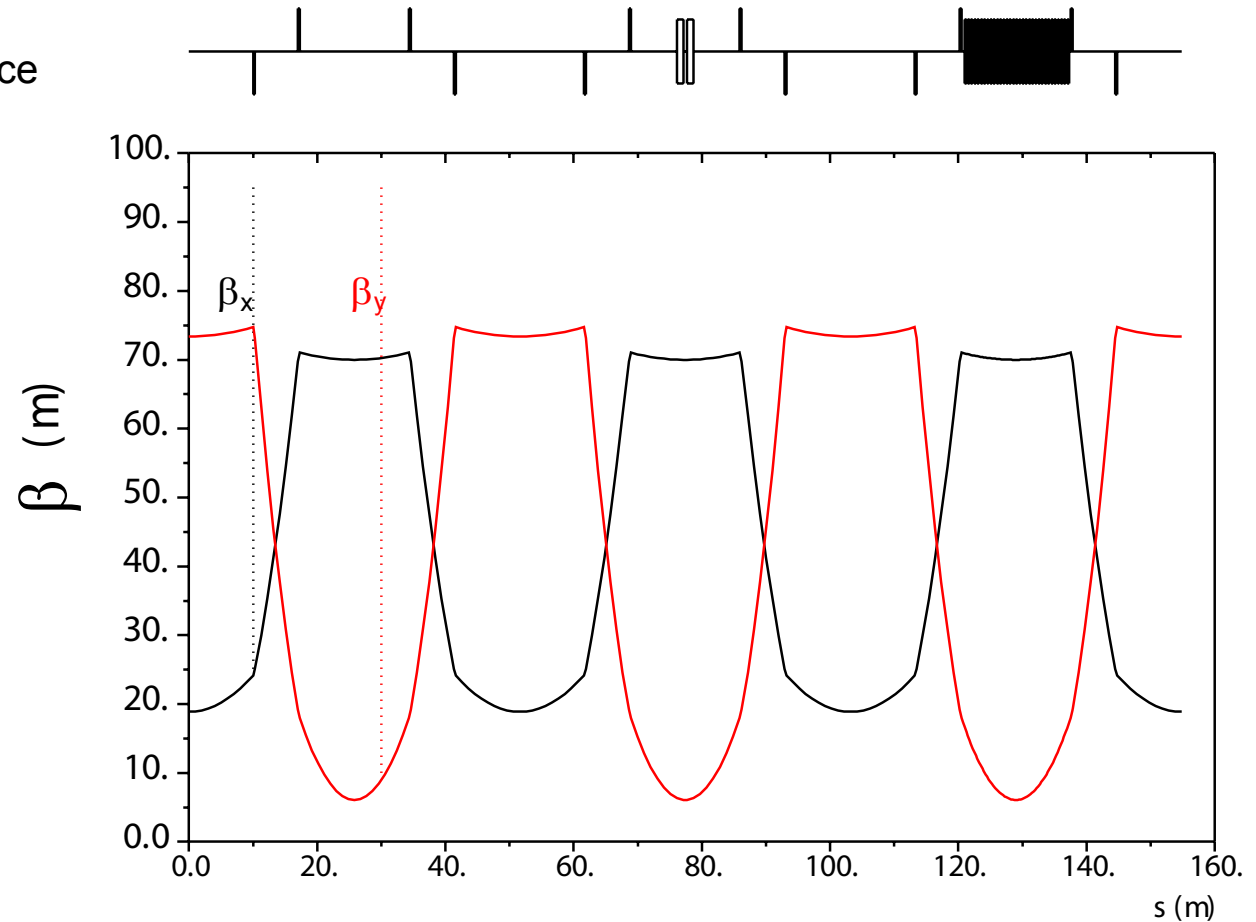


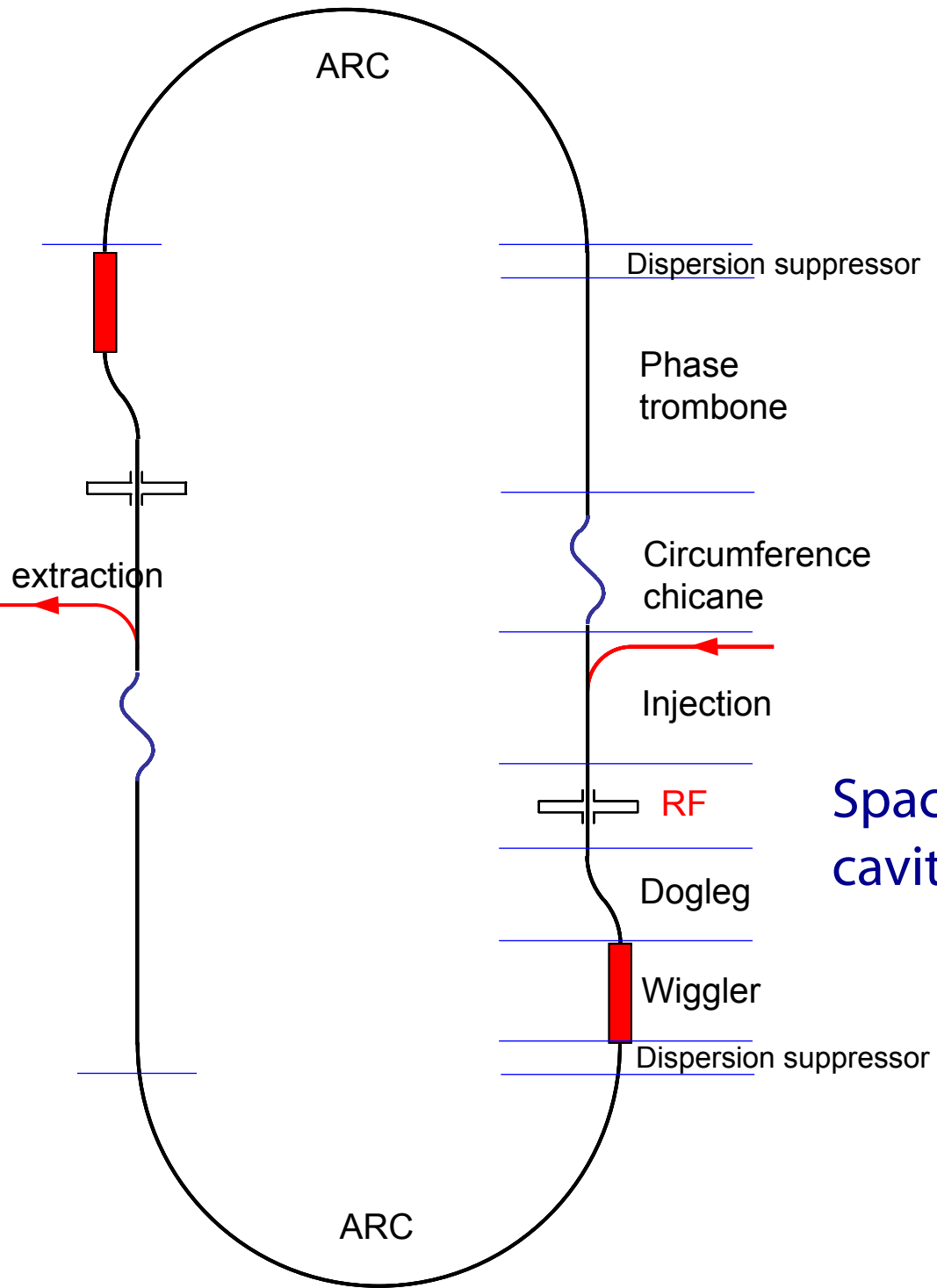
The path length around the ring may become quite sensitive to thermal or ground motion effects. A change of the path length will cause a change in both the beam energy and the closed orbit. Thus, to restore and control the nominal path length the circumference chicane is required.

Total range of circumference adjustability ± 8 mm.

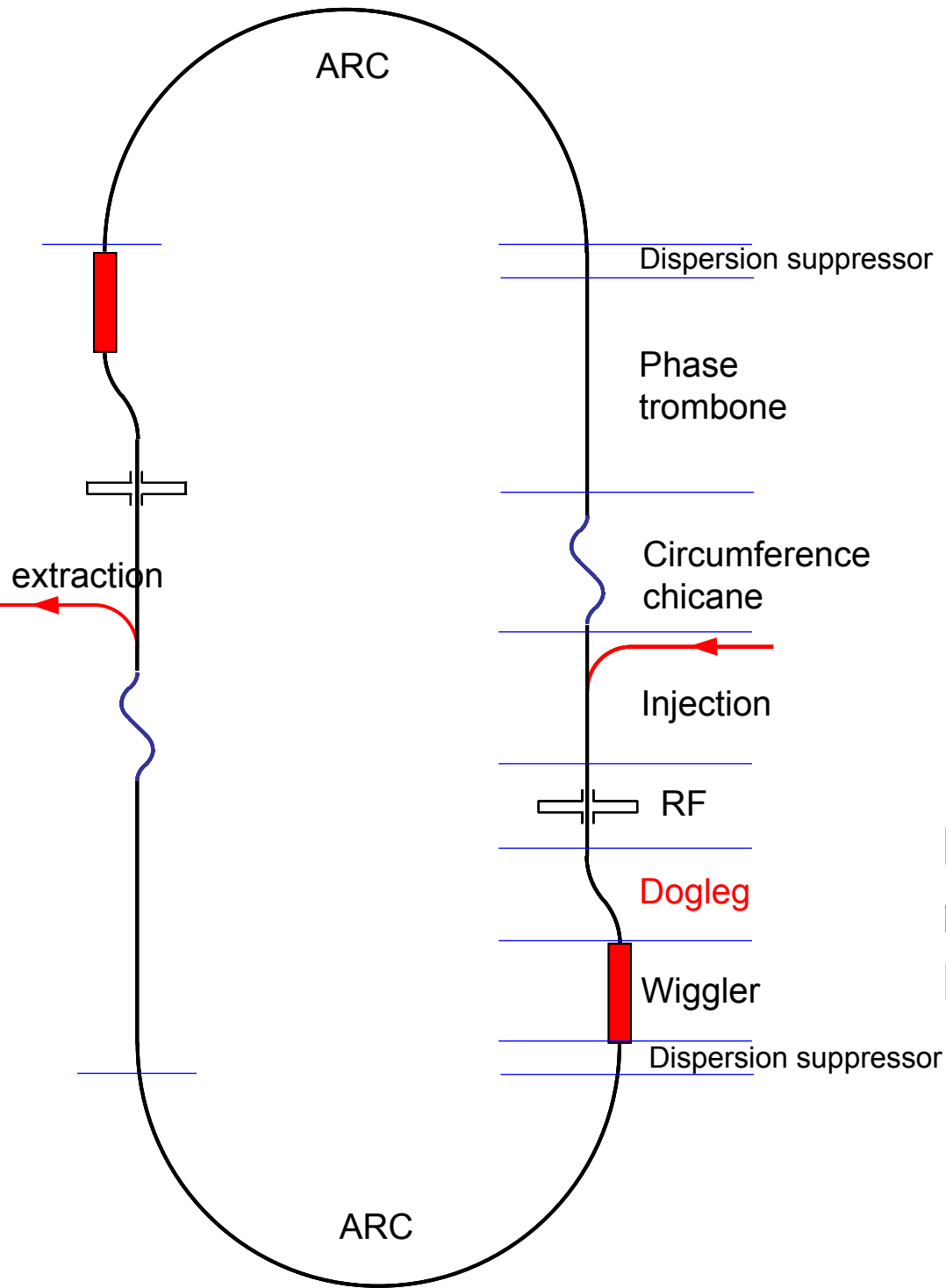


- Injection and extraction optics are similar to each other.
- Symmetry around septum provides possibility for closed orbit bumps.
- High beta function gives low phase advance over kickers, and large beam offset at septum.
- Space for 33 kicker "modules" (assuming 30 cm striplines with 20 cm separation). With 30 kickers operational, pulzers must supply ± 7 kV.

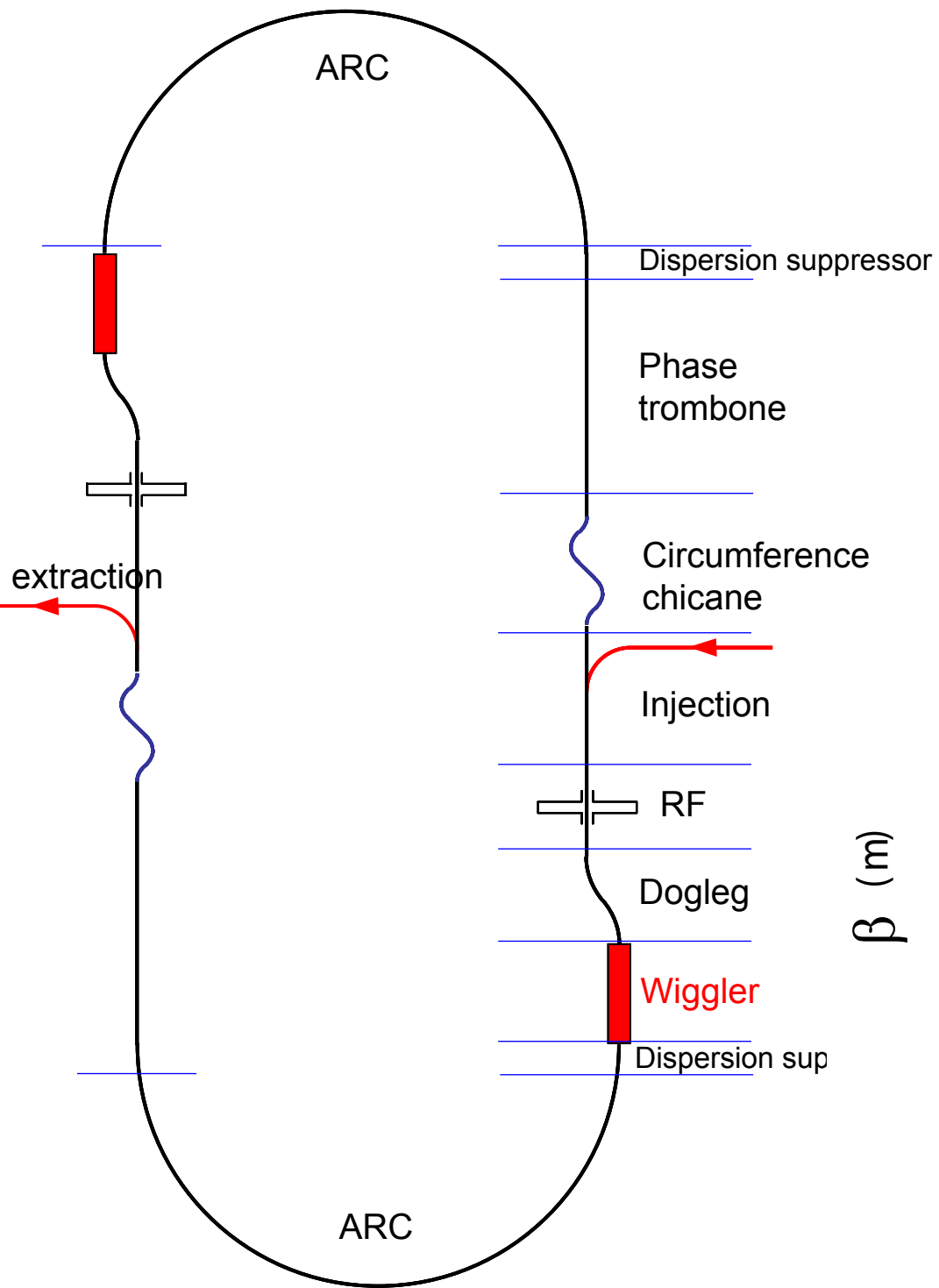




Space available for 24 rf superconducting cavities (12 per straight)

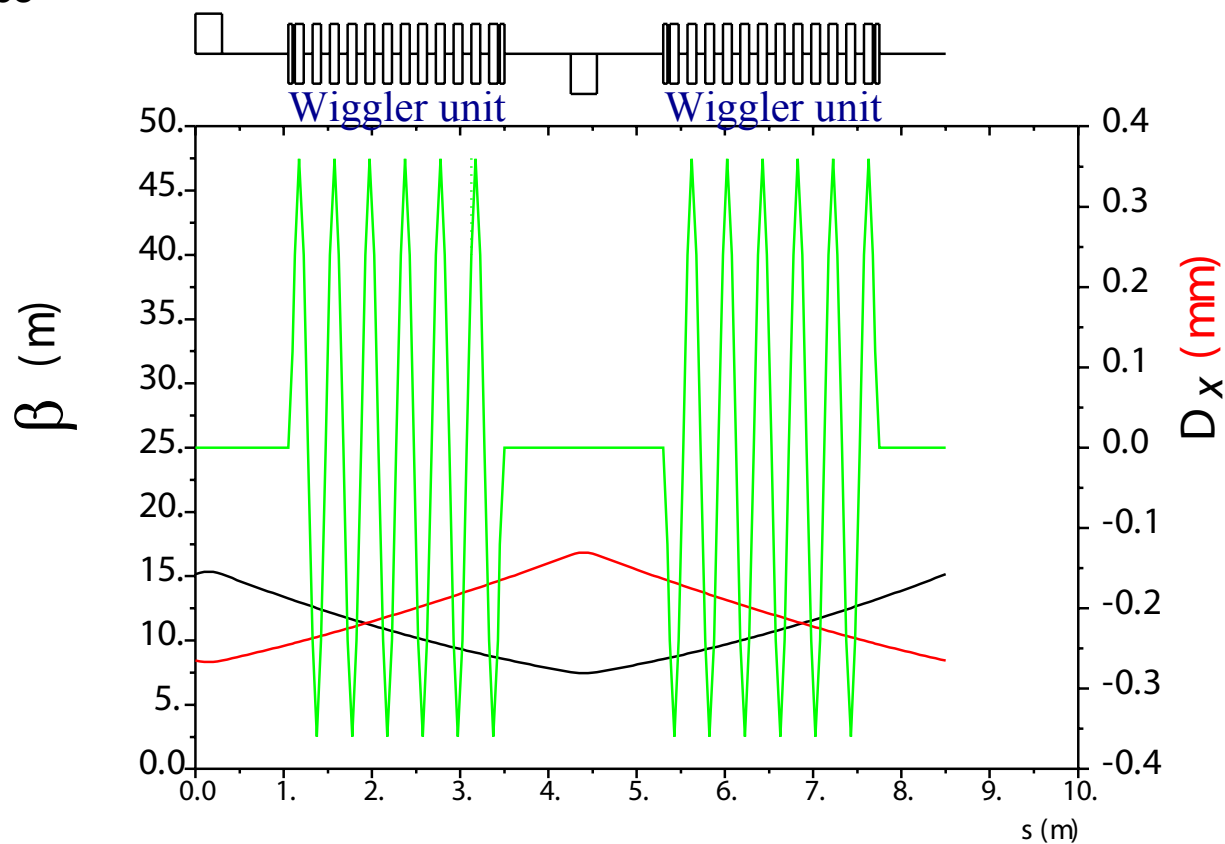


Dogleg gives horizontal separation of roughly 2 m, between the wiggler and RF sections.



88 superconducting wiggler magnets in the ring

Wiggler type	Superconducting
Wiggler peak field	1.6 T
Wiggler period	0.4 m
Wiggler unit length	2.45 m
Wiggler total length	215.6 m



Arrangement of sextupole magnets in the arcs

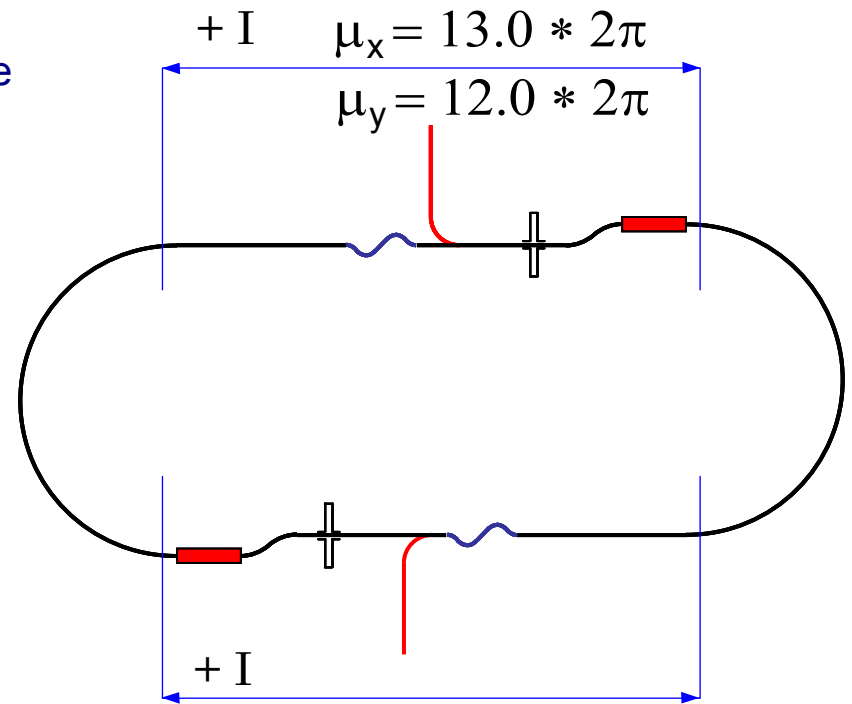
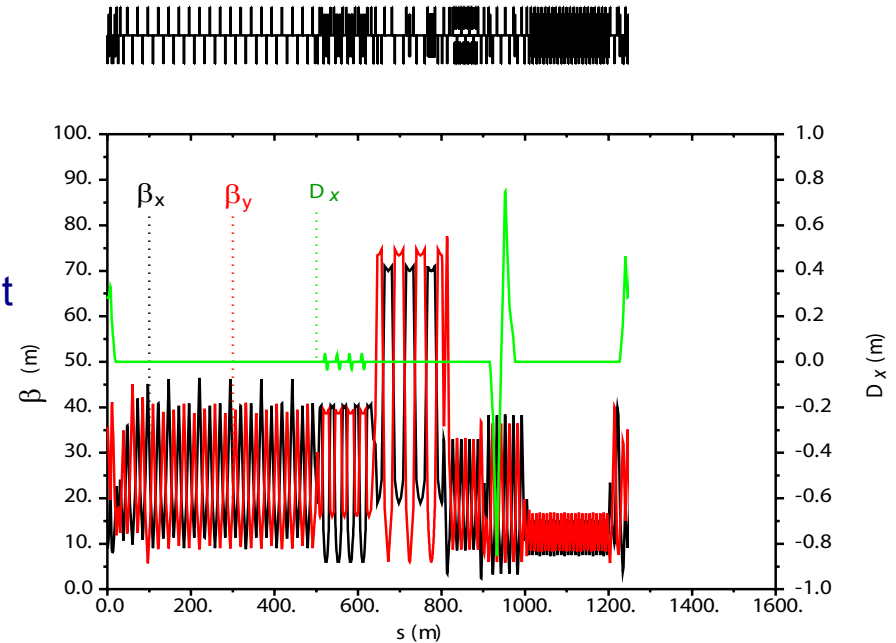
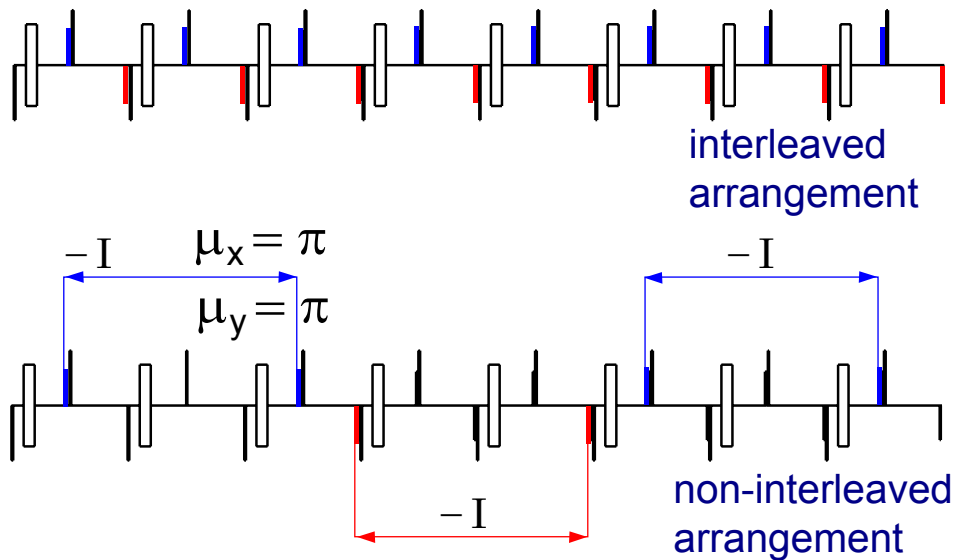
Natural chromaticity of the ring increase mainly with phase advance in the arcs.

To compensate the large natural chromaticity, two interleaved sextupole families are arranged in the arcs.

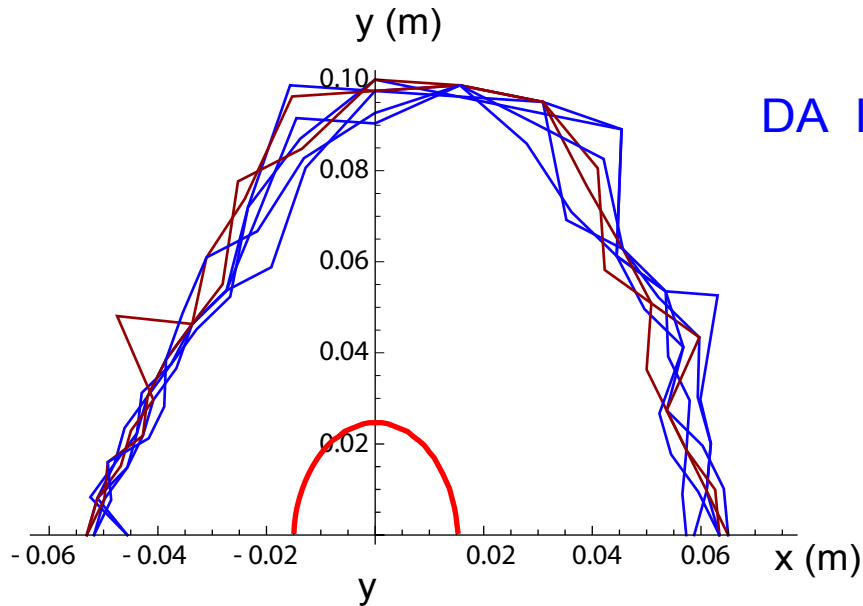
At phase advance close to 90 degree, such interleaved arrangement of the sextupole introduces strong second-order geometric aberrations which limit dynamic aperture to unacceptable value.

For the particular case when phase advance in the arc cell is close to 90 degree a non-interleaved -I arrangement of the sextupole pairs is applied.

So, for this particular phase advance a non-interleaved -I arrangement (minus unity transformation matrix) of the sextupole pairs is applied.

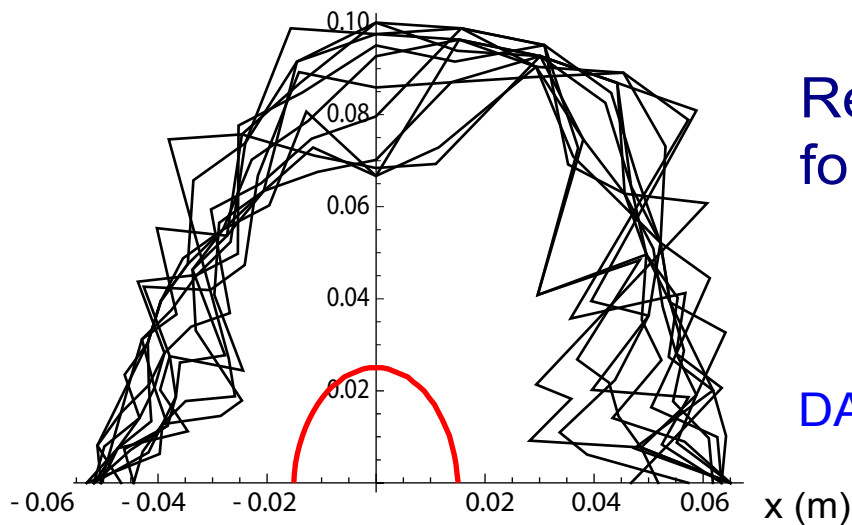


Dynamic aperture of the damping ring



DA looks acceptable for on-momentum particles

Phase advance	72 degree	90 degree	100 degree
V_x range	64.10 – 64.17	73.10 – 73.17	78.10 – 78.17
V_y range	61.15 – 61.55	70.15 – 70.45	75.40 – 75.45



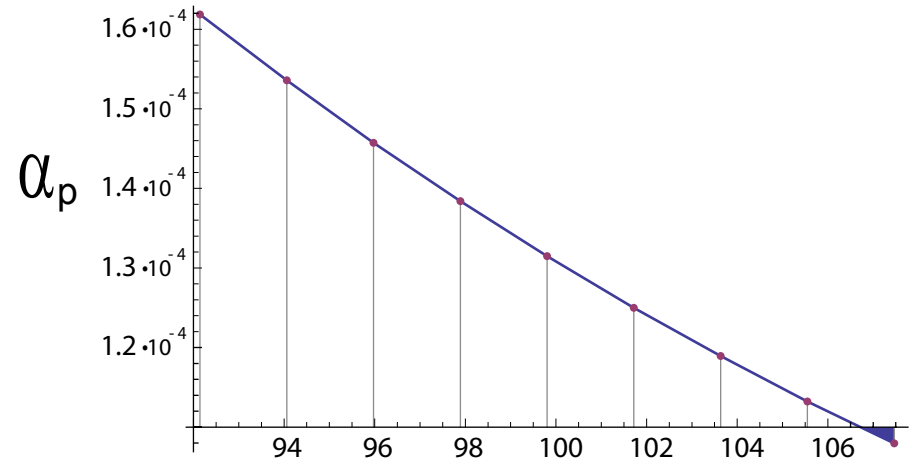
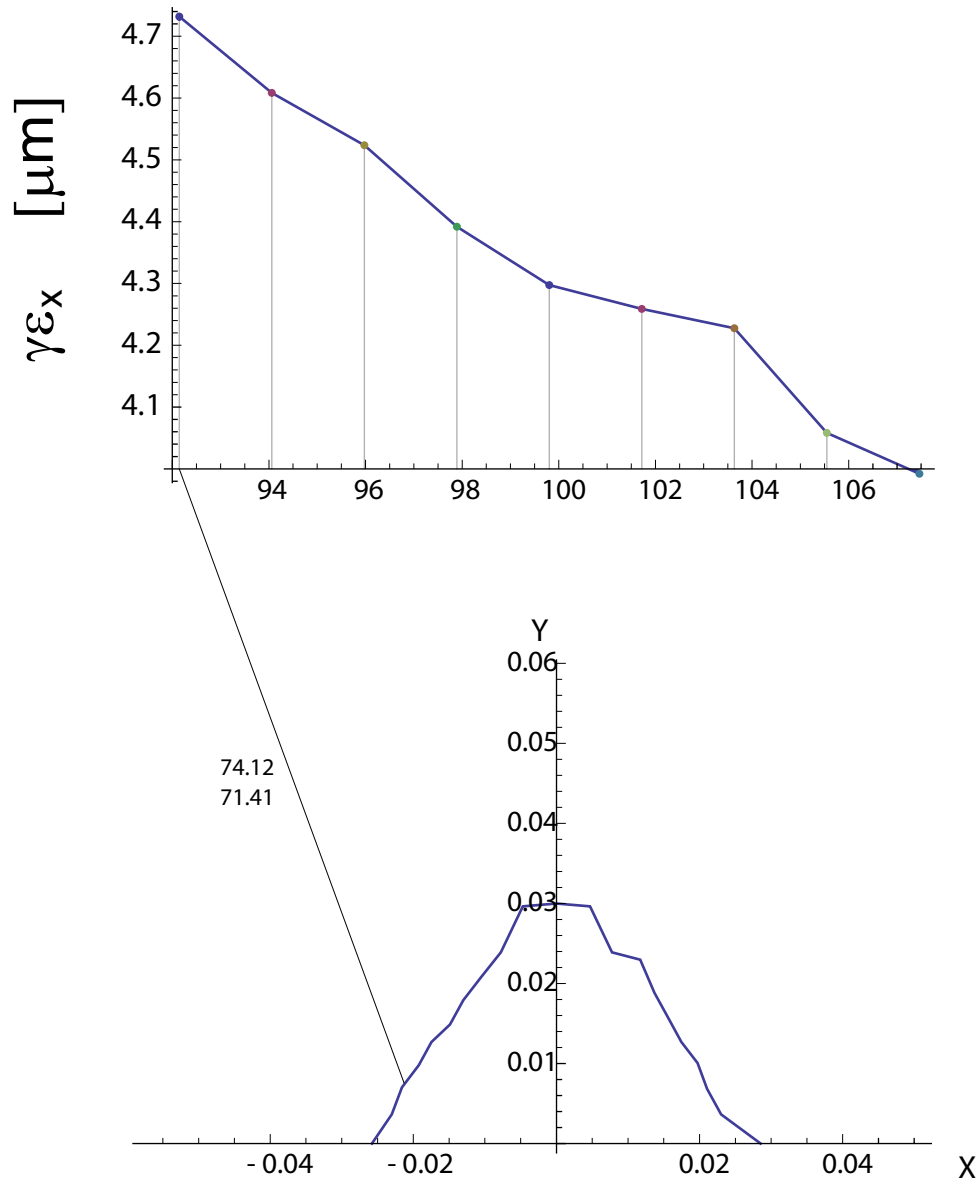
Red ellipse shows maximum particle coordinates for injected positron beam that corresponds to

$$\gamma(A_x + A_y) = 0.09 \text{ m}$$

DA looks **unacceptable**

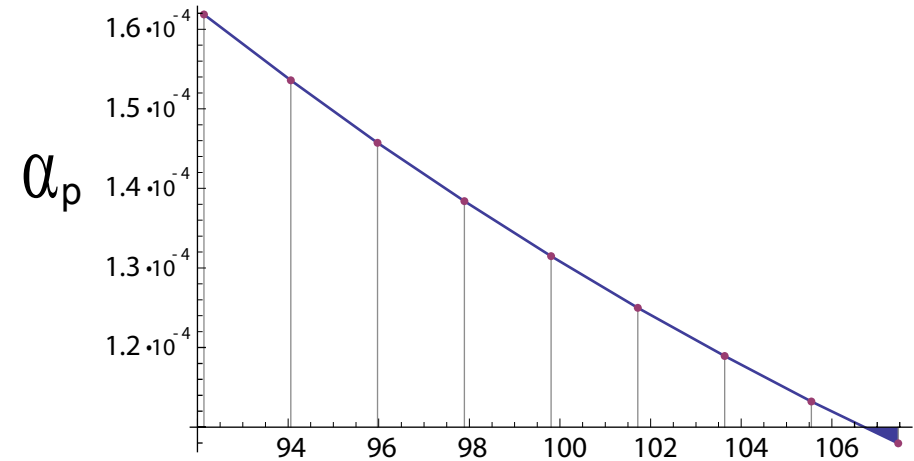
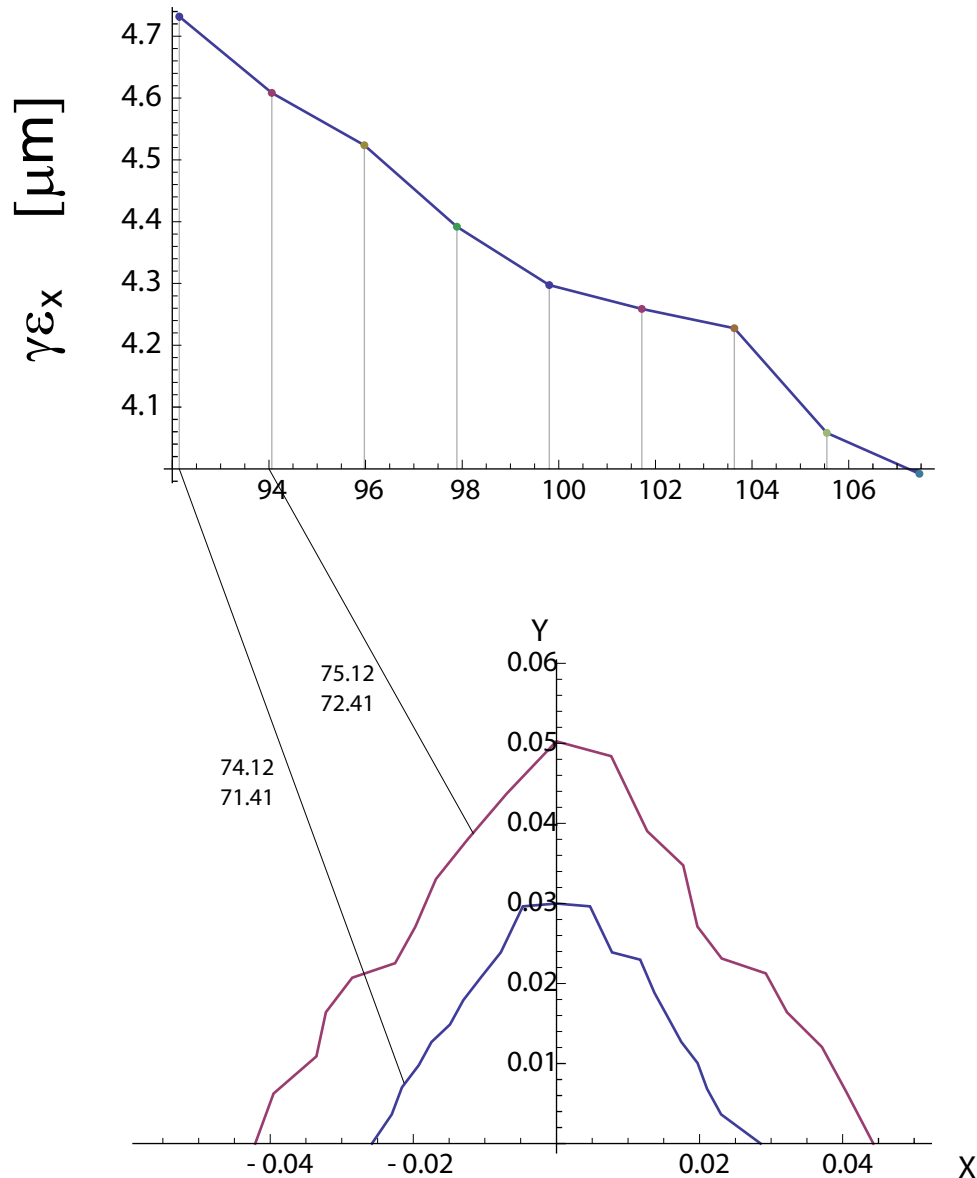
example of dynamic aperture with FODO phase advance of 72 degree

Horizontal normalized emittance and dynamic aperture as a function of horizontal phase advance in the FODO cell.



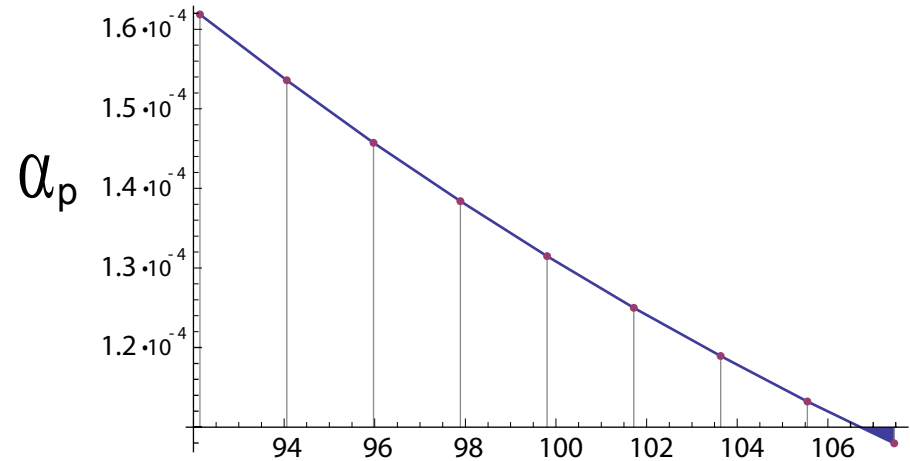
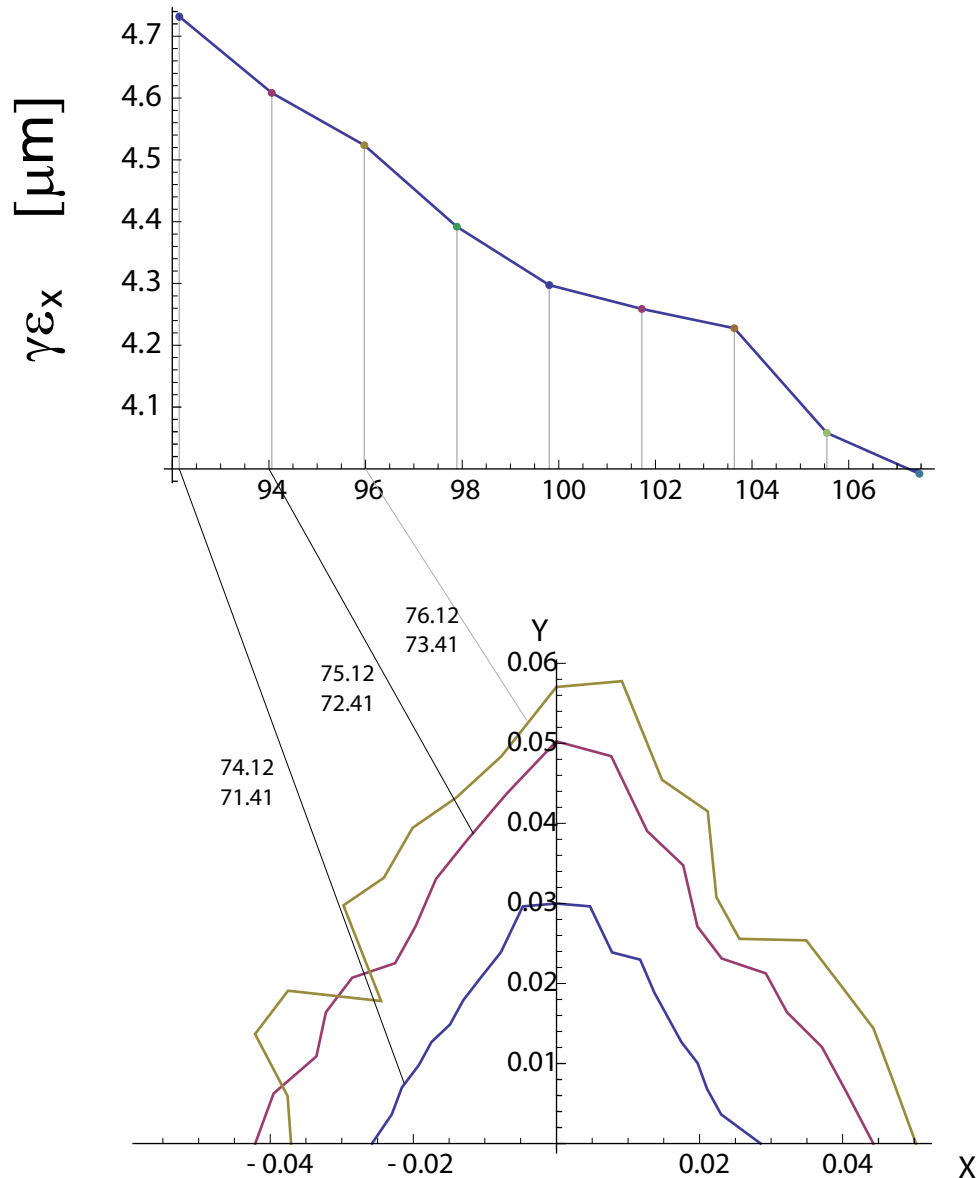
fractional parts of horizontal and vertical betatron tunes for whole ring are .12 and .41 respectively

Horizontal normalized emittance and dynamic aperture as a function of horizontal phase advance in the FODO cell.



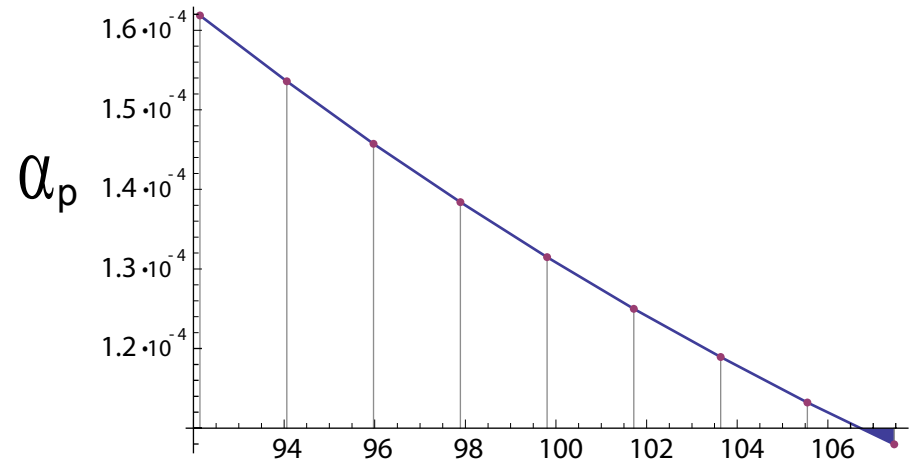
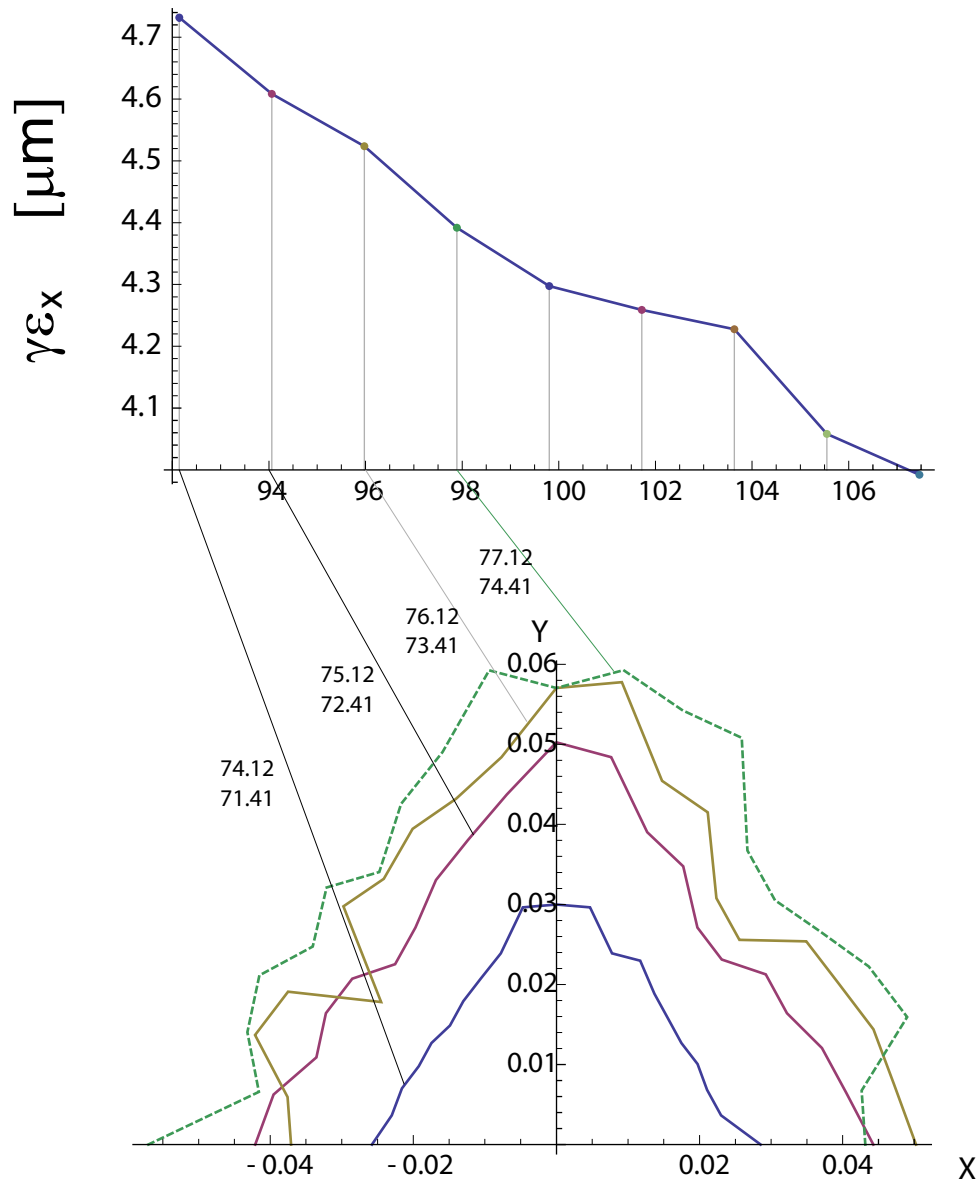
fractional parts of horizontal and vertical betatron tunes for whole ring are .12 and .41 respectively

Horizontal normalized emittance and dynamic aperture as a function of horizontal phase advance in the FODO cell.



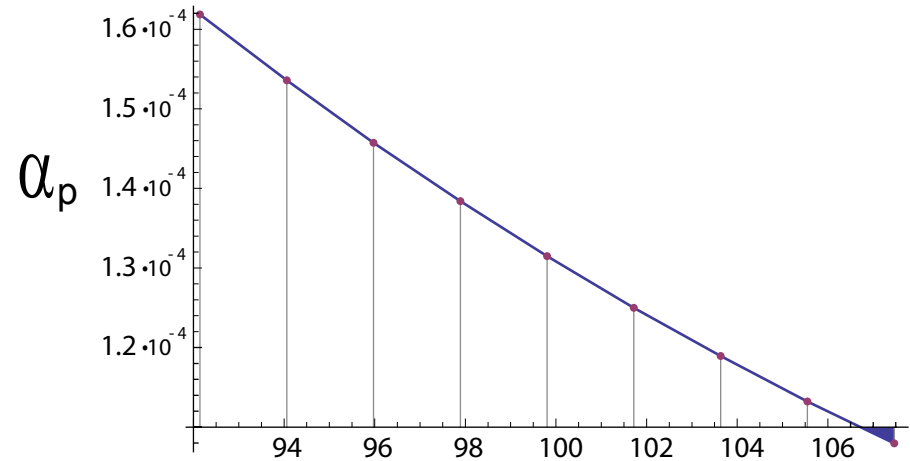
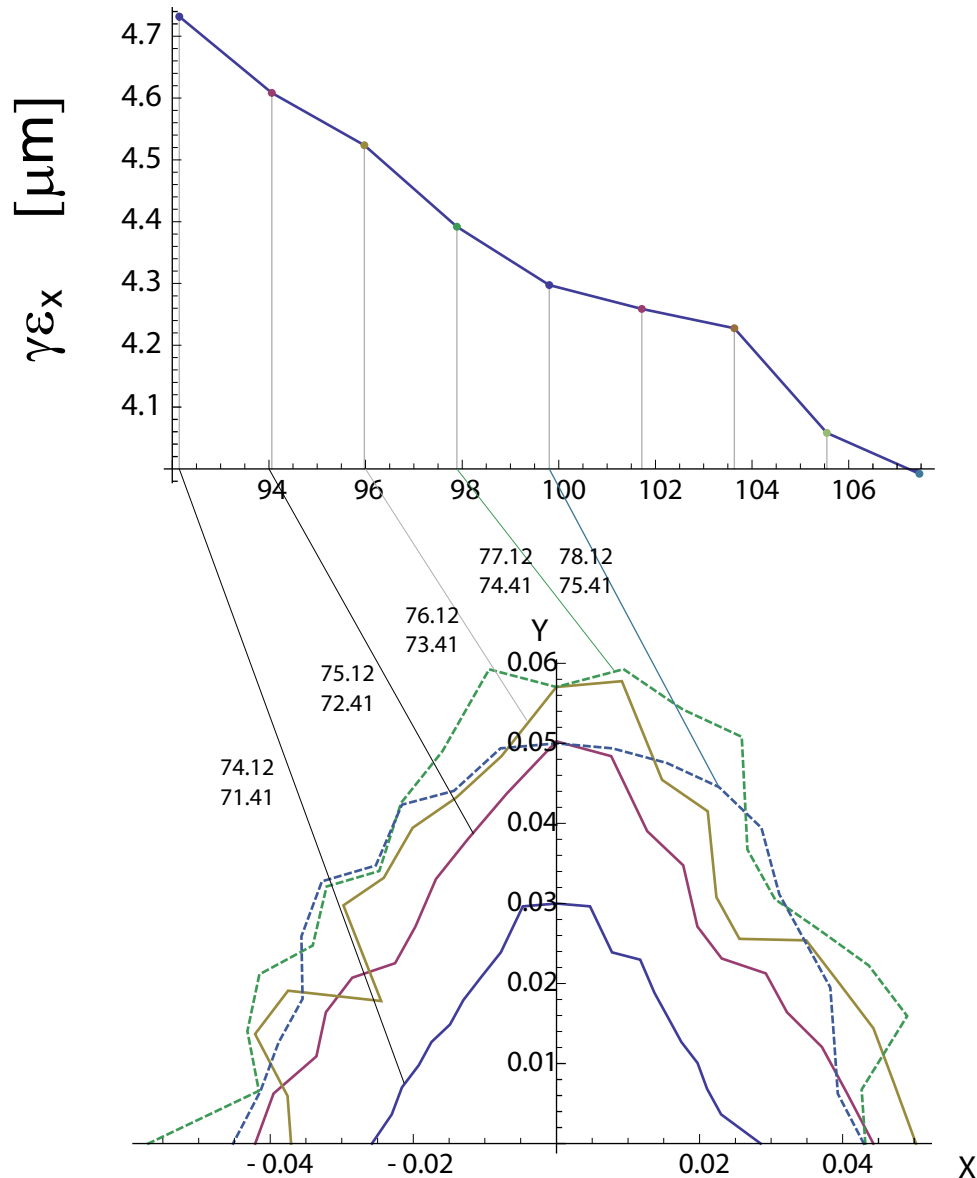
fractional parts of horizontal and vertical betatron tunes for whole ring are .12 and .41 respectively

Horizontal normalized emittance and dynamic aperture as a function of horizontal phase advance in the FODO cell.



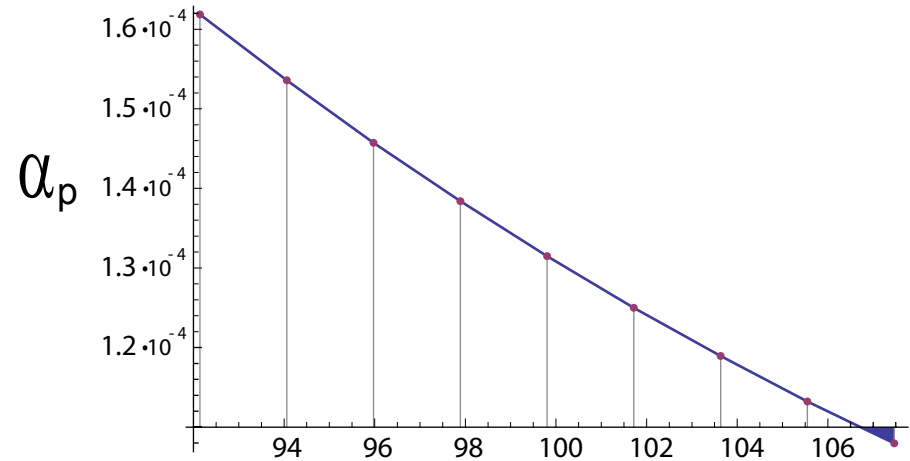
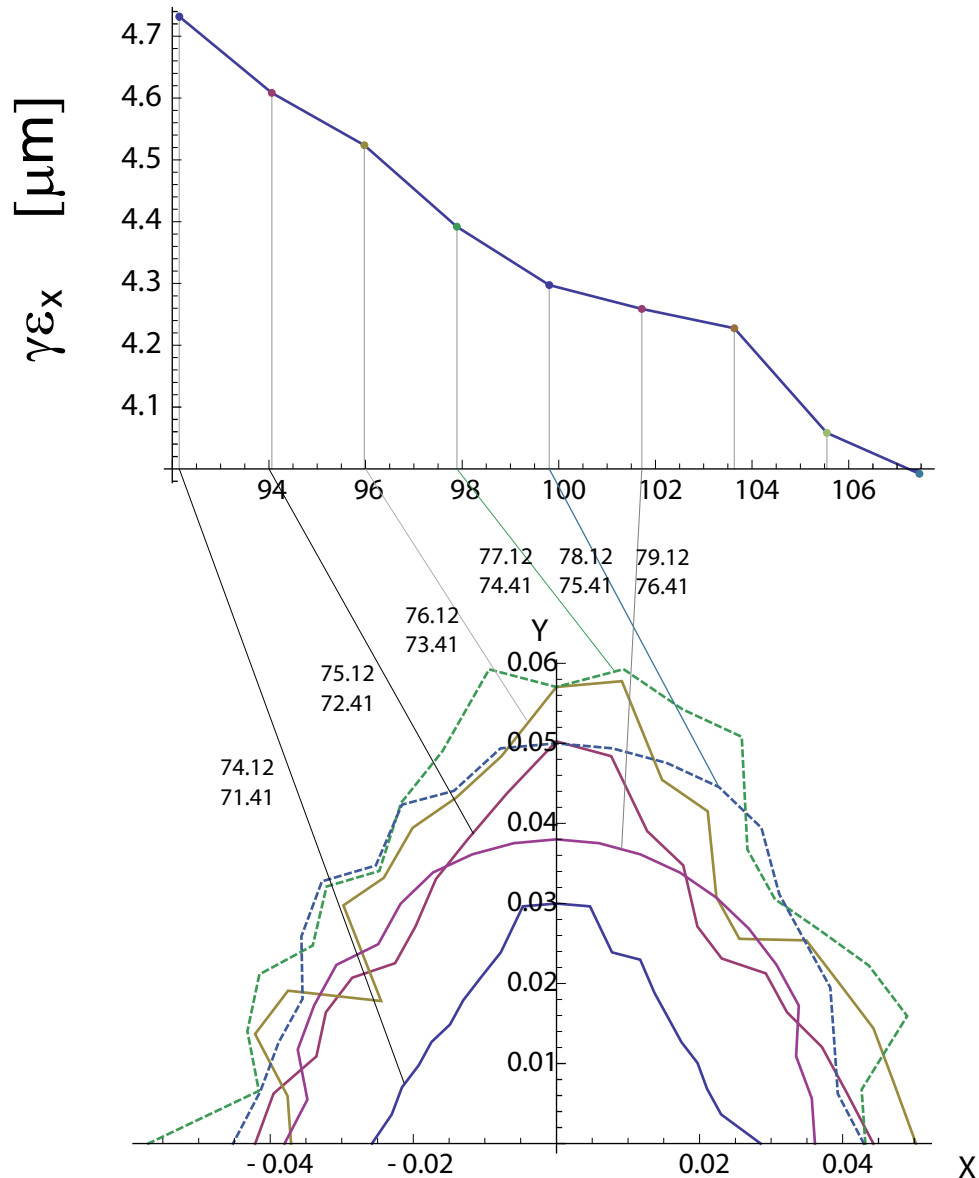
fractional parts of horizontal and vertical betatron tunes for whole ring are .12 and .41 respectively

Horizontal normalized emittance and dynamic aperture as a function of horizontal phase advance in the FODO cell.



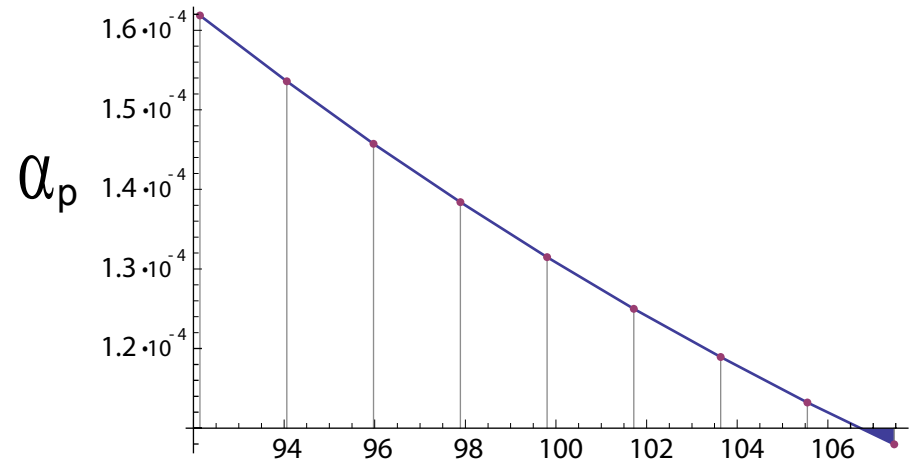
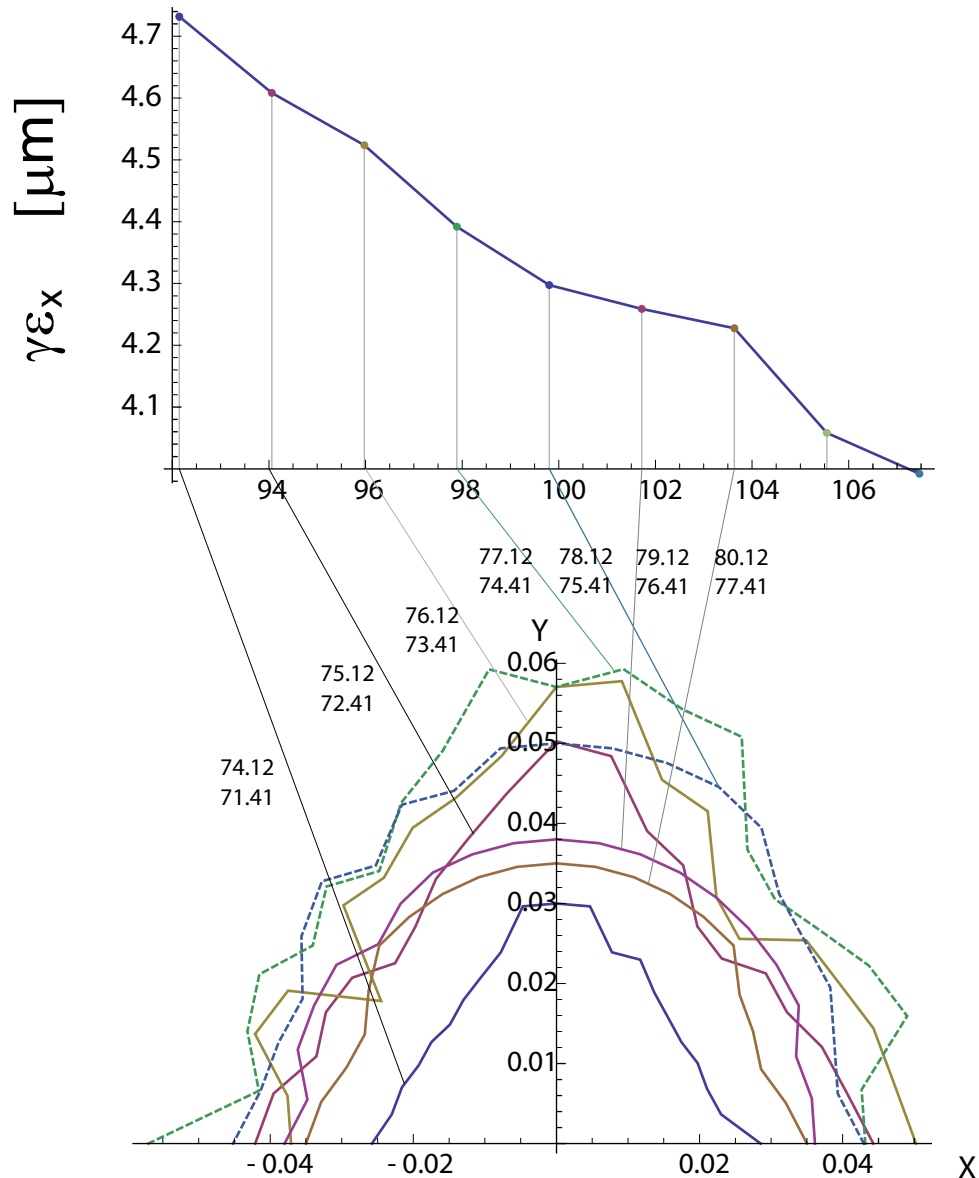
fractional parts of horizontal and vertical betatron tunes for whole ring are .12 and .41 respectively

Horizontal normalized emittance and dynamic aperture as a function of horizontal phase advance in the FODO cell.



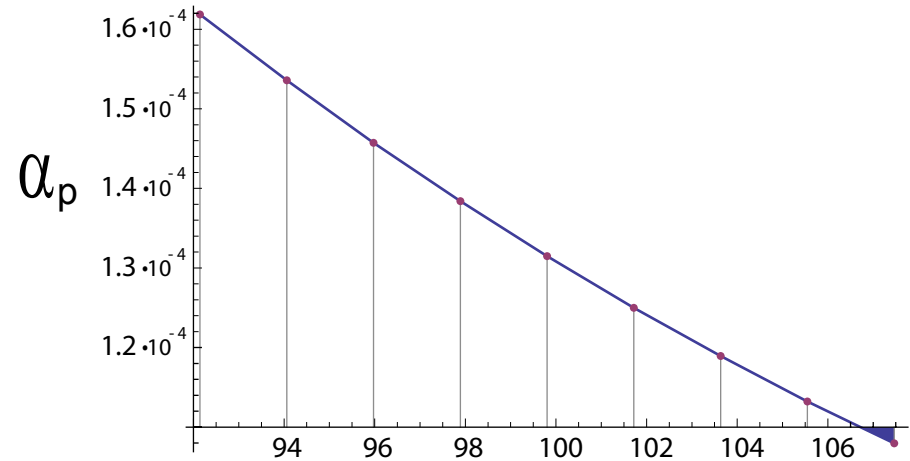
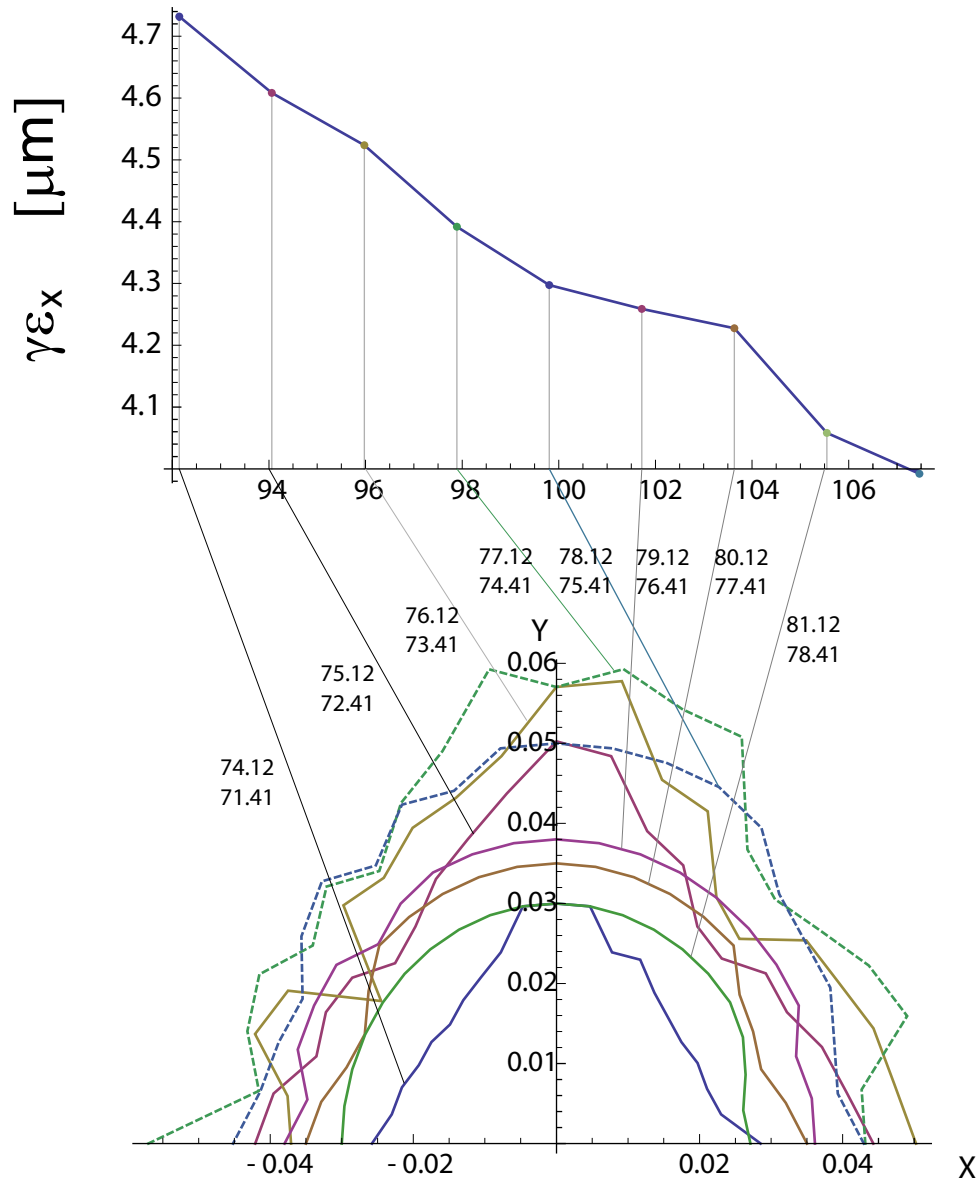
fractional parts of horizontal and vertical betatron tunes for whole ring are .12 and .41 respectively

Horizontal normalized emittance and dynamic aperture as a function of horizontal phase advance in the FODO cell.



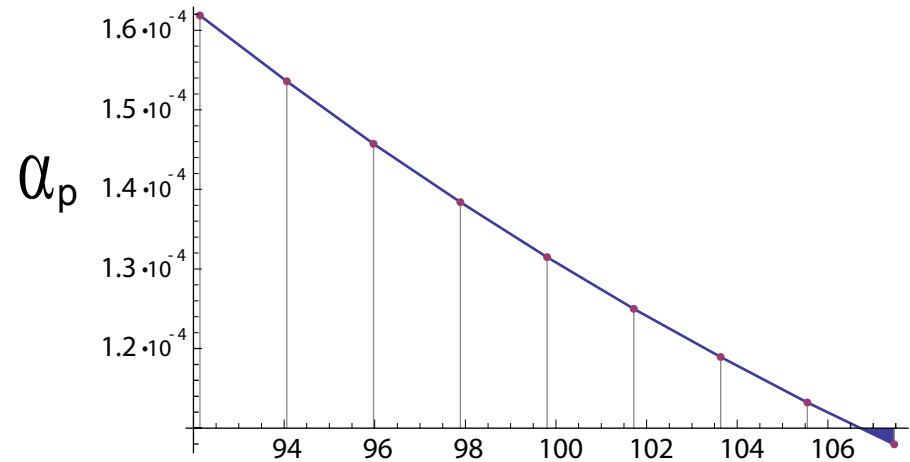
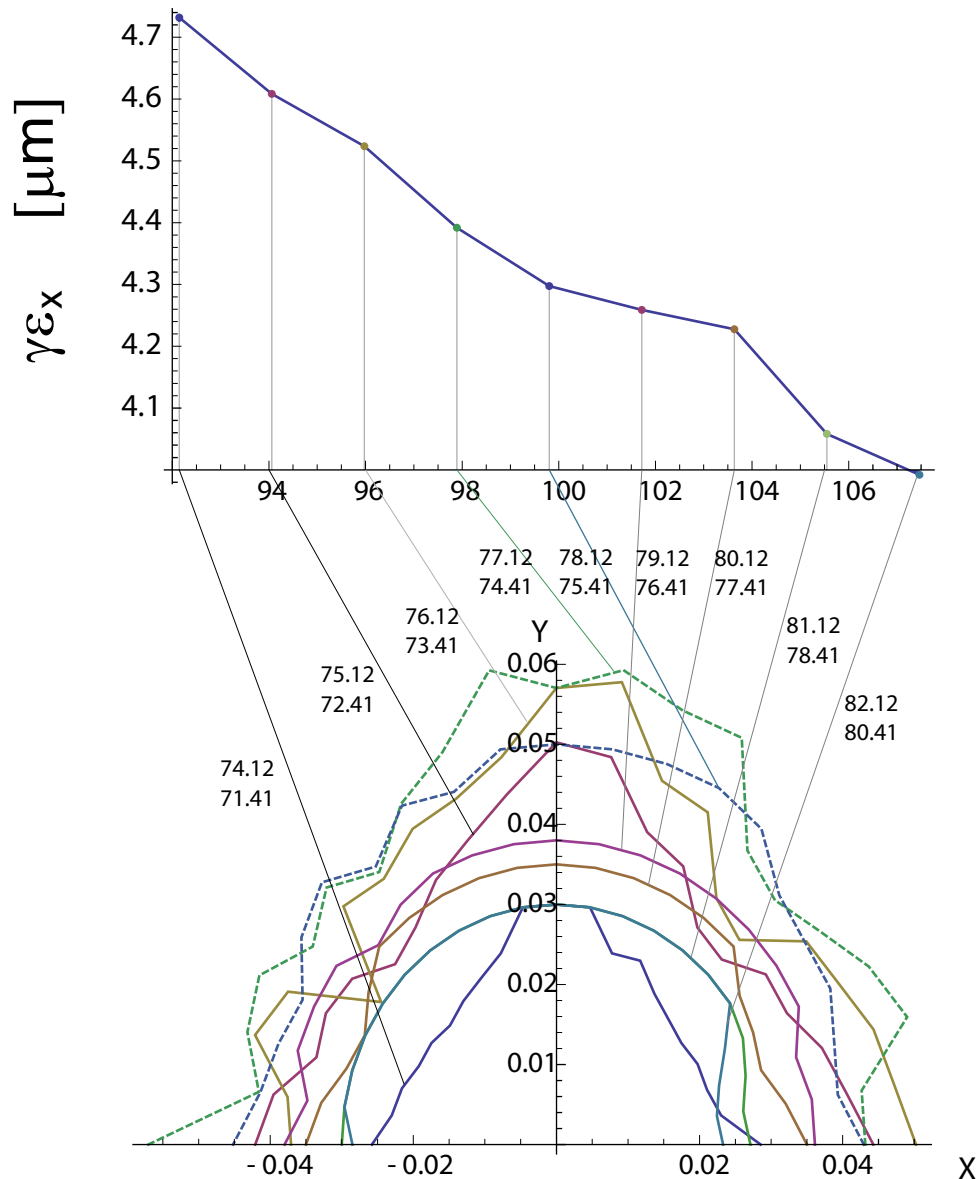
fractional parts of horizontal and vertical betatron tunes for whole ring are .12 and .41 respectively

Horizontal normalized emittance and dynamic aperture as a function of horizontal phase advance in the FODO cell.



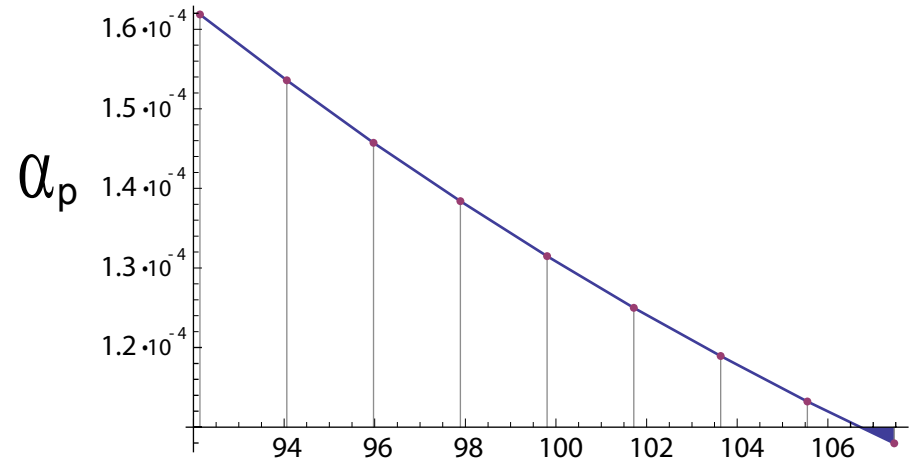
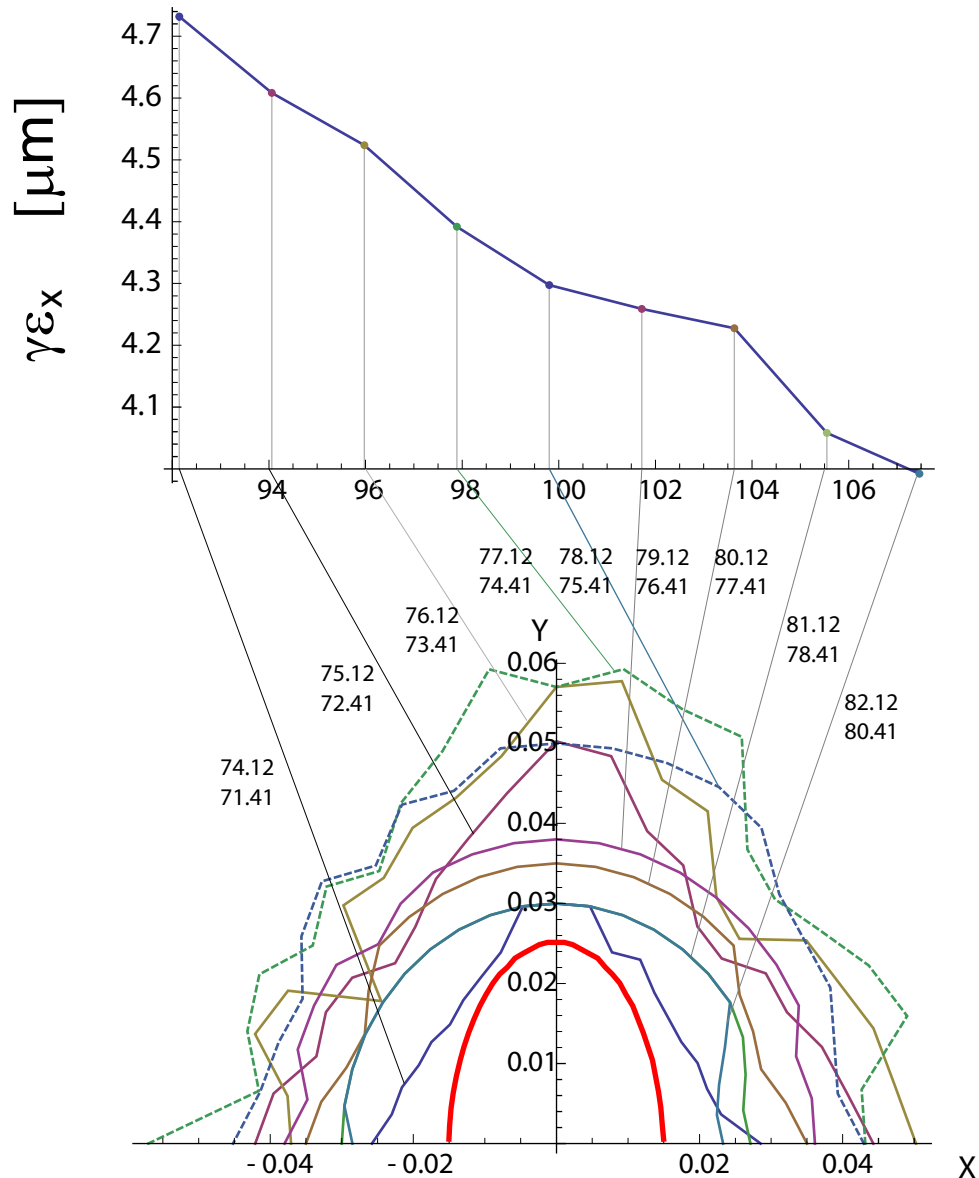
fractional parts of horizontal and vertical betatron tunes for whole ring are .12 and .41 respectively

Horizontal normalized emittance and dynamic aperture as a function of horizontal phase advance in the FODO cell.



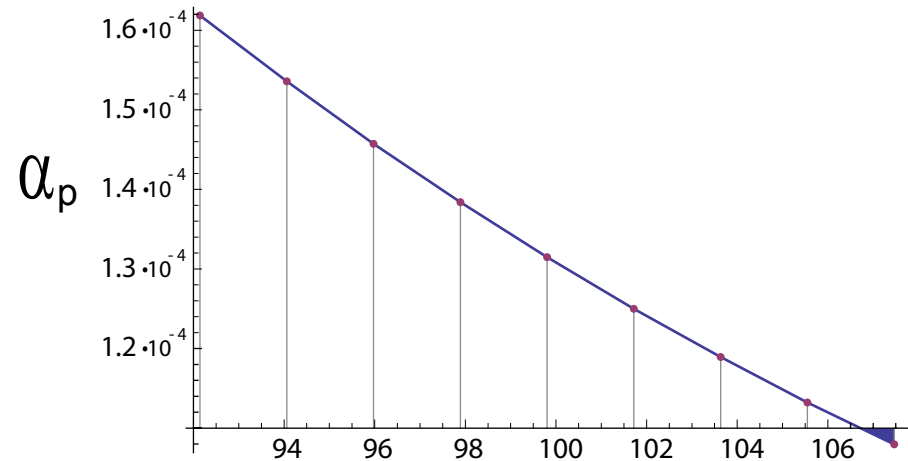
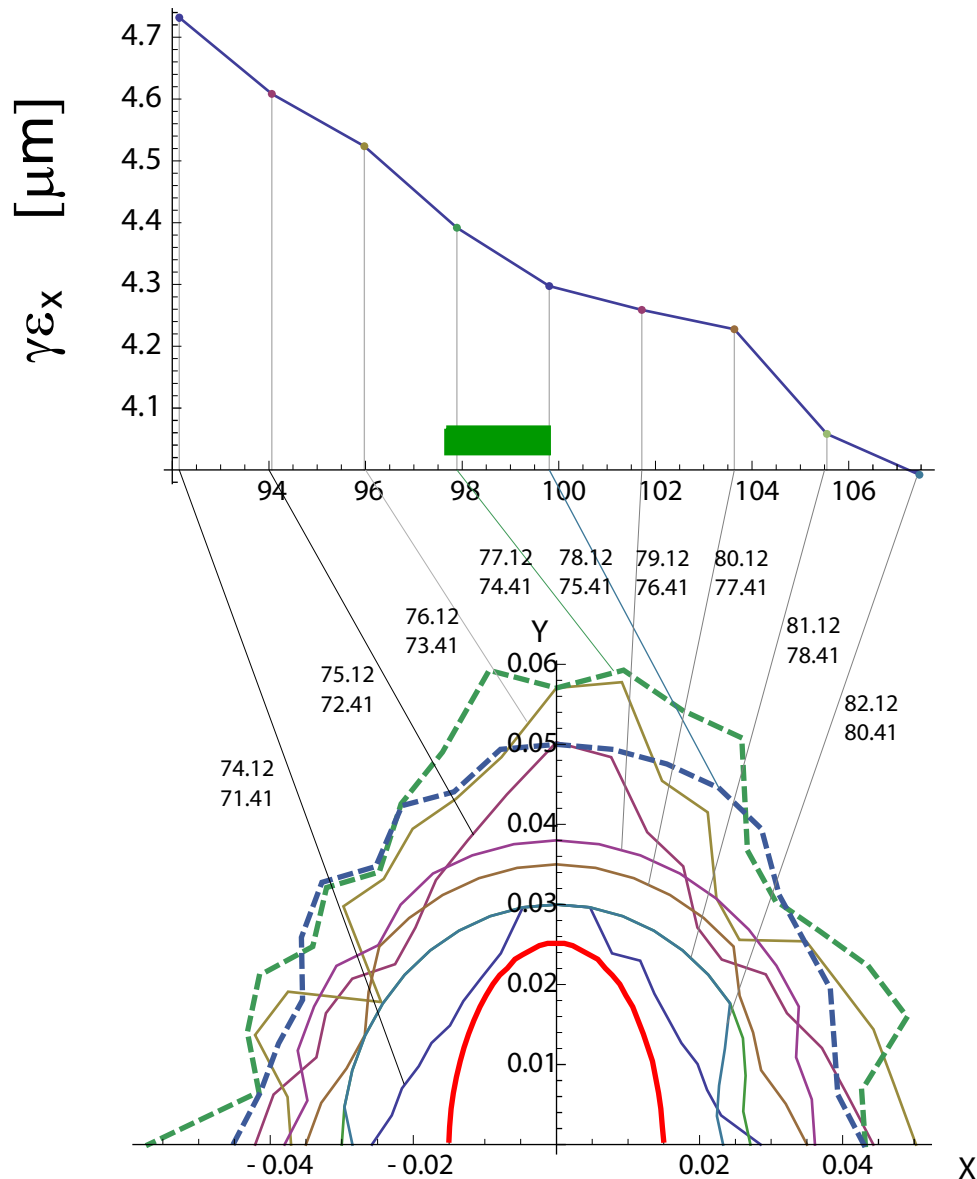
fractional parts of horizontal and vertical betatron tunes for whole ring are .12 and .41 respectively

Horizontal normalized emittance and dynamic aperture as a function of horizontal phase advance in the FODO cell.



fractional parts of horizontal and vertical betatron tunes for whole ring are .12 and .41 respectively

Horizontal normalized emittance and dynamic aperture as a function of horizontal phase advance in the FODO cell.



fractional parts of horizontal and vertical betatron tunes for whole ring are .12 and .41 respectively

Low Emittance Tuning for the ILC Damping Rings

Goals :

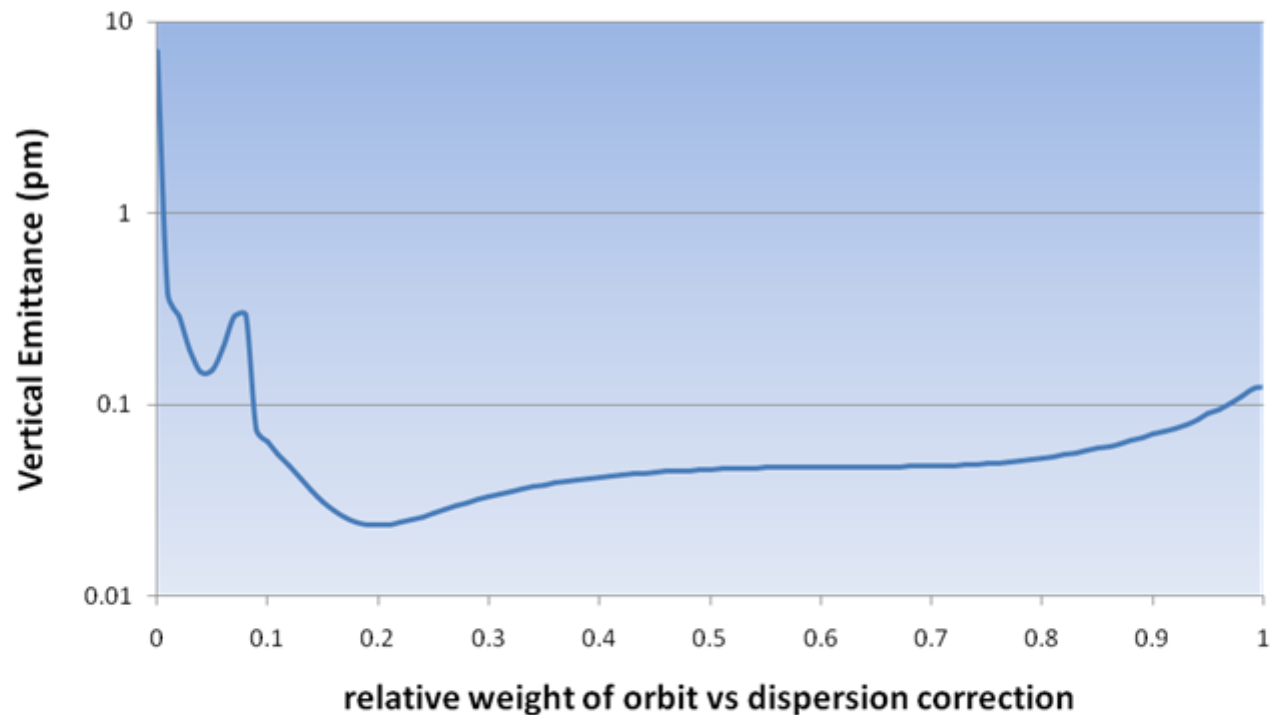
To develop a good understanding of sensitivities to various errors

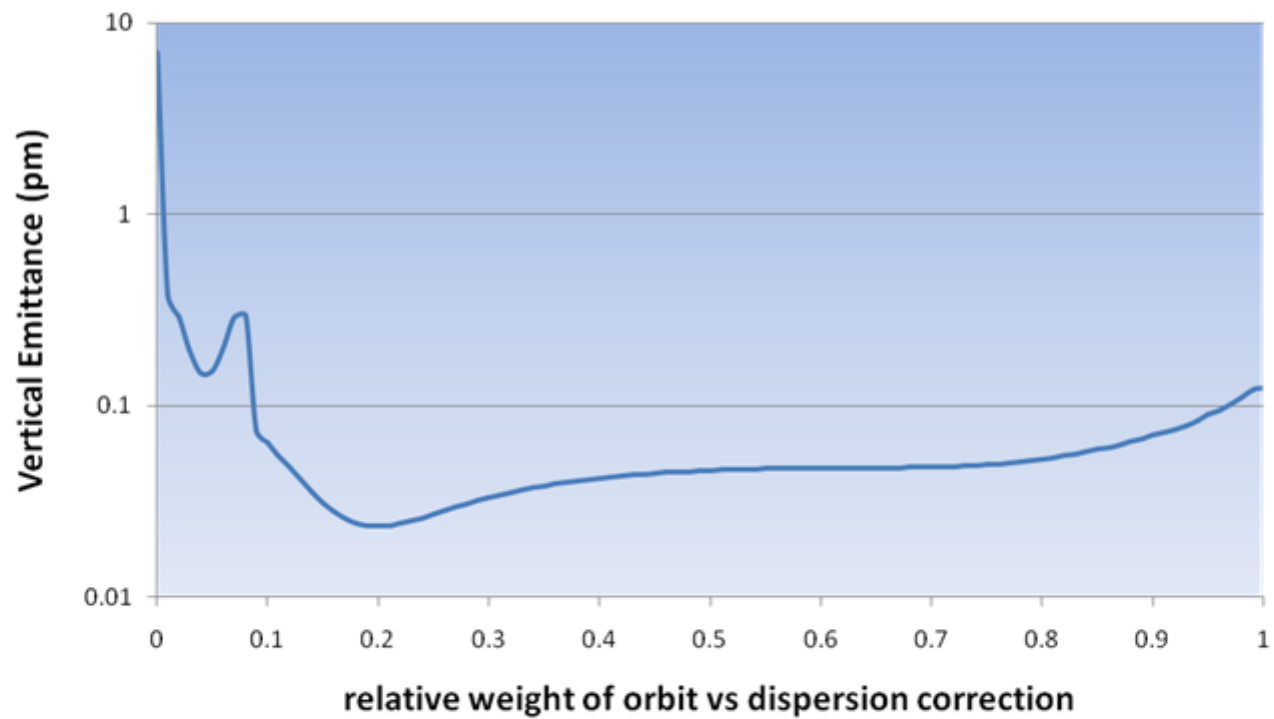
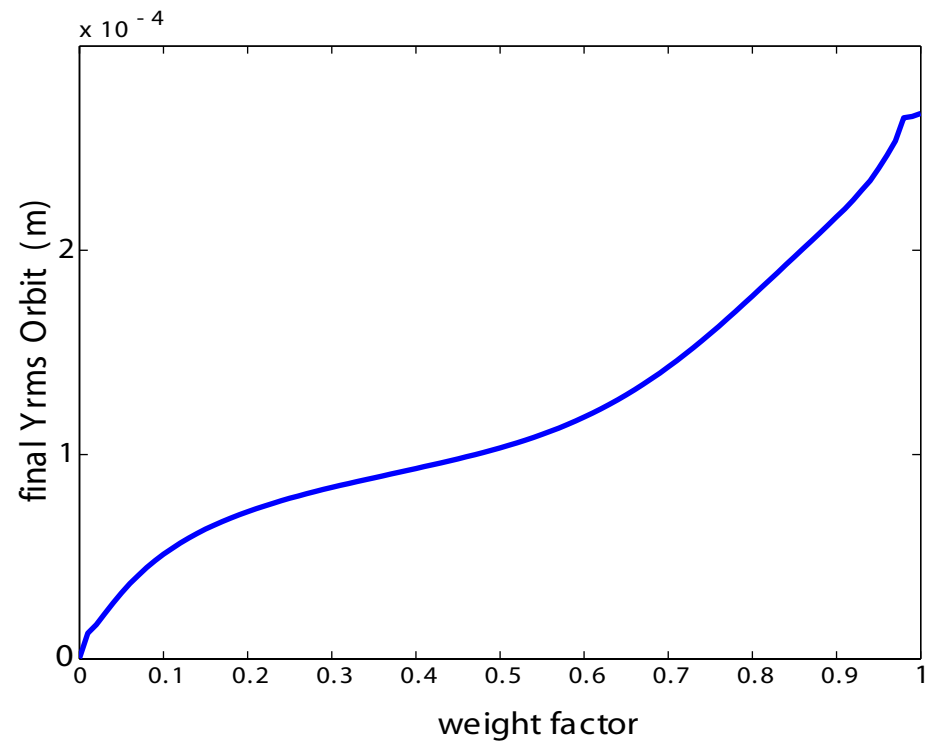
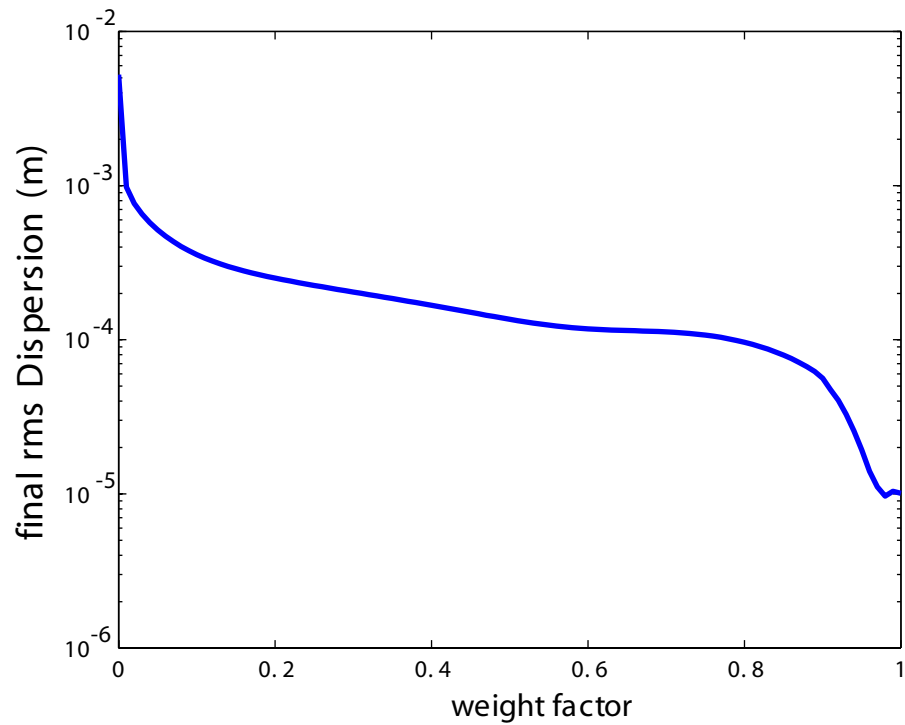
To compare and optimize a range of tuning procedures

To optimize design of coupling correction system

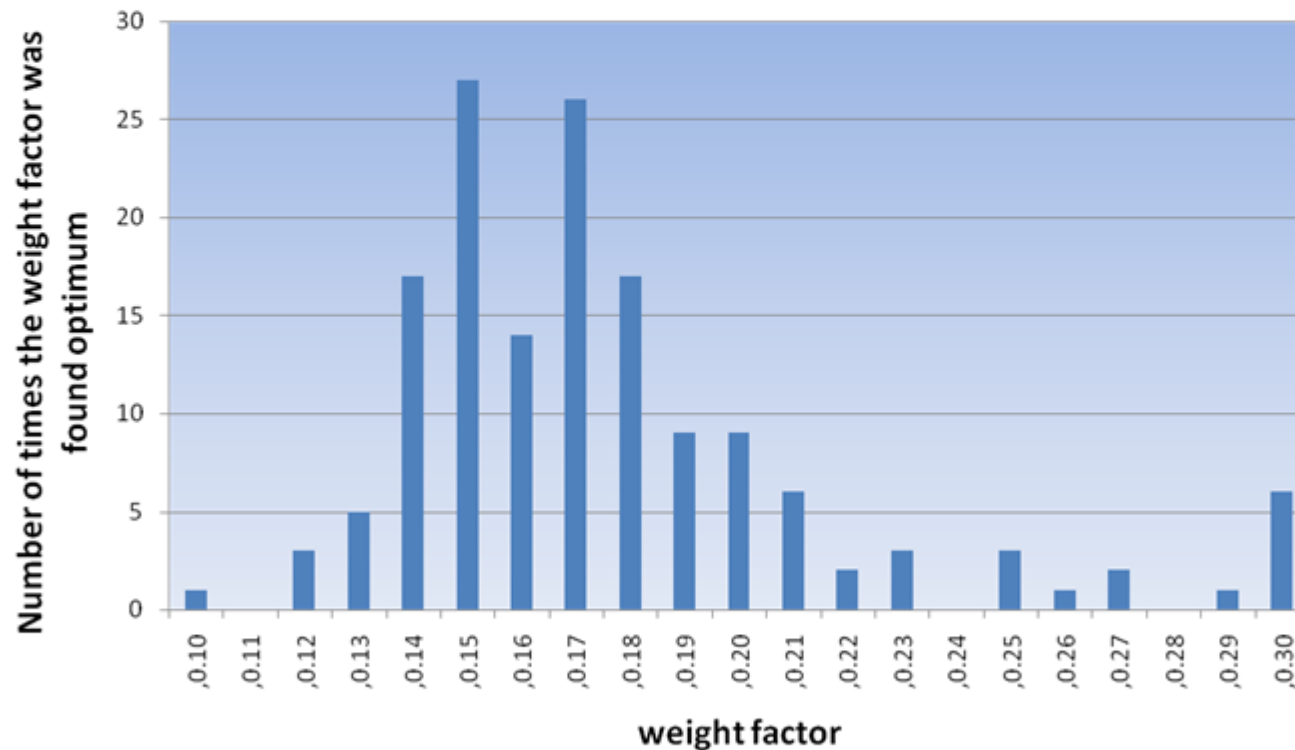
$$\begin{pmatrix} (1-\alpha)\vec{u} \\ \alpha\vec{D}_u \end{pmatrix} + \begin{pmatrix} (1-\alpha)\mathbf{A} \\ \alpha\mathbf{B} \end{pmatrix} \vec{\theta} = 0 \Rightarrow S = (1-\alpha)^2 \|\vec{u} + \mathbf{A}\vec{\theta}\|^2 + \alpha^2 \|\vec{D}_u + \mathbf{B}\vec{\theta}\|^2 \rightarrow \min$$

- Since orbit and dispersion cannot each be perfectly corrected at the same time, we have to choose to weight one relative to the other.
- A weight factor equal to 0 reflects a fully corrected orbit and uncorrected dispersion and vice versa for a weight factor equal to 1.

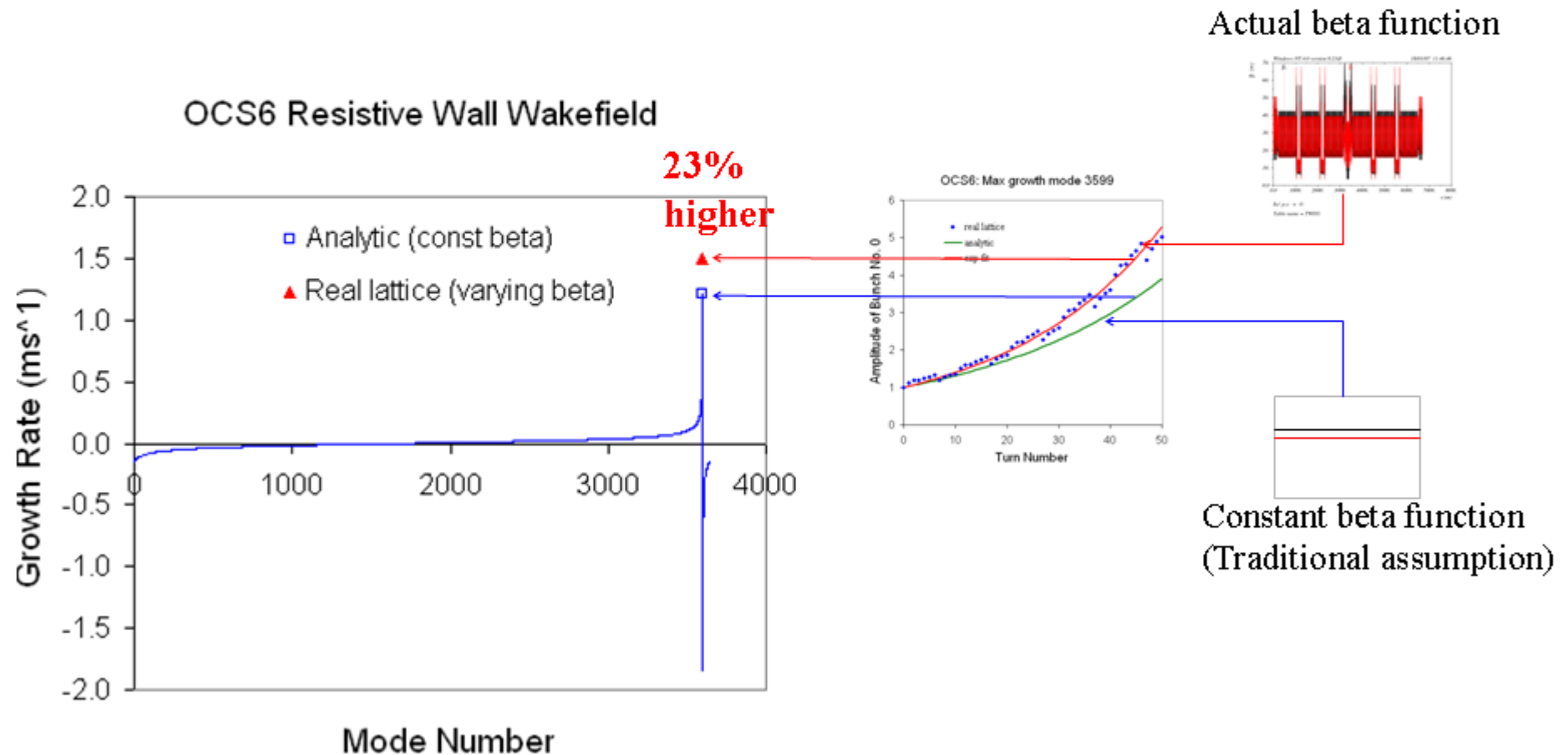




- The aim is to find the optimum value for the weight factor (which is the value that minimizes the emittance).
- Running the same simulation for a number of random sets of errors we can statistically determine the optimum weight factor .



Transverse coupled bunches



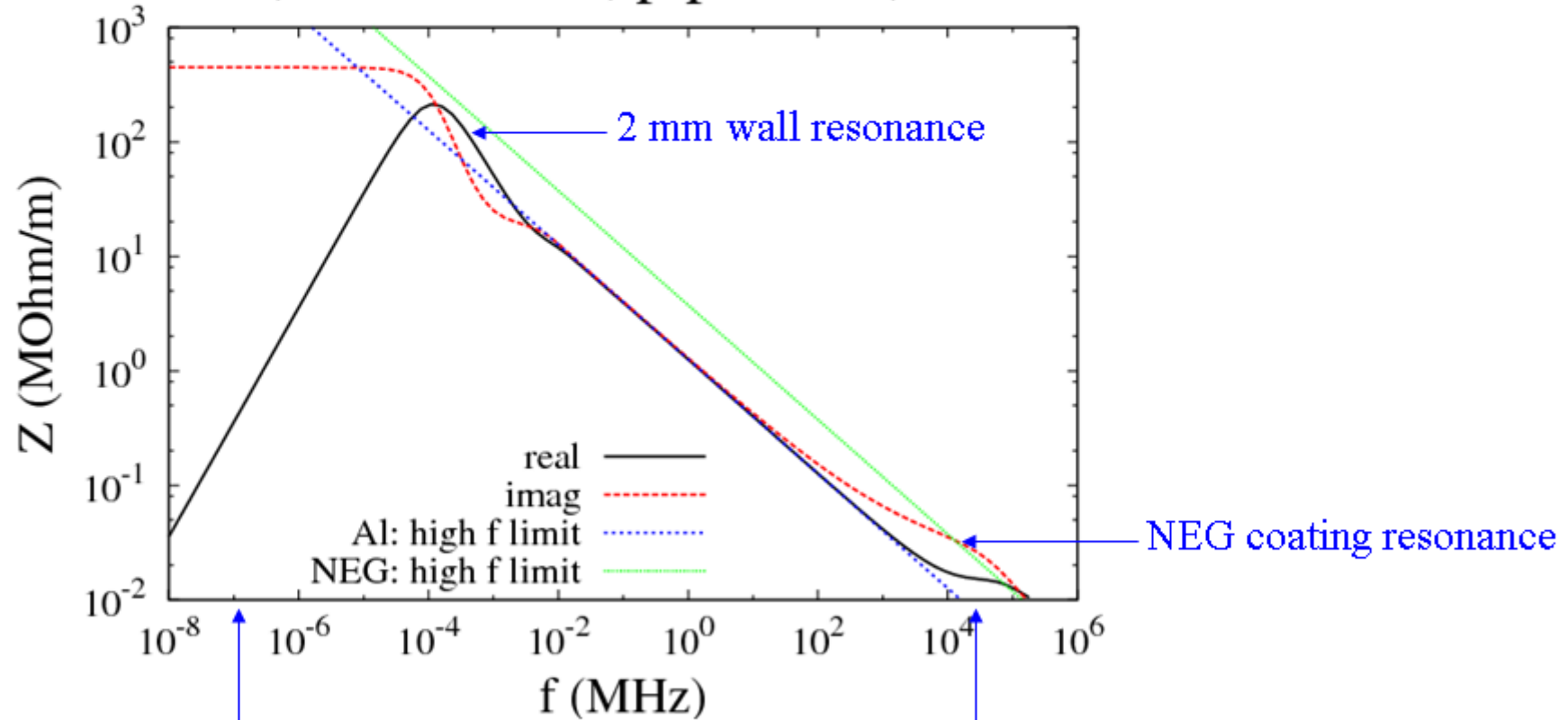
Hock and Wolski, Phys. Rev. ST AB 10, 084401 (2007)

Resistive wall impedance can cause exponential growth of transverse amplitude.

The growth rate calculated by standard formulae that assumes a constant (monotonic) beta functions and growth rates calculated for actual beta functions of the ring is shown

NEG coating impedance

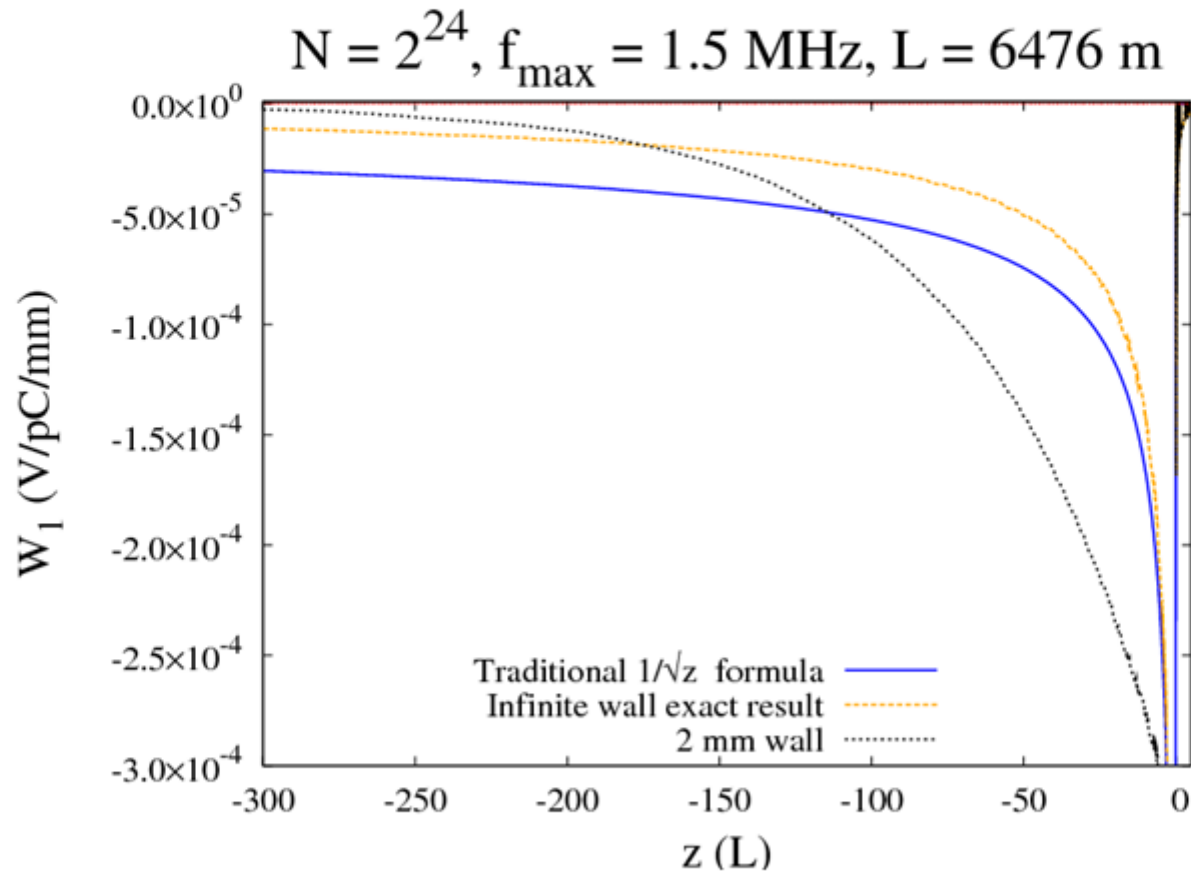
wall 2 mm, beam 3 mm, pipe 3 cm, NEG = 1 μm



f_{min} for sum of
Wake fields to converge

f_{max} to cover the
minimum bunch spacing

Finite wall wake function



- blue curve: standard resistive wall wake field formula for infinitely thick wall.
- orange curve: correct wake field for infinitely thick wall
- black: wake field for 2 mm thick wall.

Summary

Lattice design

- meets specifications for principal parameters; energy, circumference, natural emittance, energy spread

Dynamic aperture

- looks reasonable but more accurate simulation is still needed

Low Emittance Tuning

- weight factor has been optimized for the simultaneous correction of vertical dispersion and orbit by using dipole correctors.

Transverse wall impedance

- to compute the effect of NEG coating, the code to allow for finite wall thickness has been developed. Then it was modified for a multilayer wall.